Why it is Difficult to Solve Helmholtz Problems with Classical Iterative Methods

Oliver G. Ernst and Martin J. Gander

1 Introduction

We consider in this paper the iterative solution of linear systems of equations arising from the discretization of the *indefinite Helmholtz equation*,

$$\mathscr{L}u := -(\Delta + k^2)u = f, \tag{1}$$

with suitable boundary conditions in order to obtain a well-posed problem. For $k > 0$ solutions of the Helmholtz equation, also known as the *reduced wave equation*, describe the variation in space of linear propagating waves with wave number k. The performance of standard iterative methods is much worse for such problems than for the deceivingly similar looking equation

$$-(\Delta - \eta)u = f, \qquad \eta > 0, \tag{2}$$

which describes stationary reaction-diffusion phenomena but is often also called Helmholtz equation in certain communities. For example in meteorology, the early seminal papers [48, 56] led an entire community to call equations of the form (2) Helmholtz equations, see for example [14]. Even standard texts in applied mathematics now sometimes use the term Helmholtz equation for both (1) and (2), see for example [66]. The subject of this paper is exclusively the indefinite Helmholtz equation (1), which is much harder to solve with classical iterative methods than equation (2).

Oliver G. Ernst
TU Bergakademie Freiberg, Institut für Numerische Mathematik und Optimierung, 09596 Freiberg, Germany e-mail: ernst@math.tu-freiberg.de

Martin J. Gander
University of Geneva, Section of Mathematics, 2-4 Rue du Lievre, CP 64, 1211 Geneva 4, Switzerland e-mail: martin.gander@unige.ch

Discretizations of the indefinite Helmholtz equation (1) using, e.g., finite differences or a finite element or spectral element method and appropriate boundary conditions result in a linear system of equations

$$A\mathbf{u} = \mathbf{f}, \tag{3}$$

which, for k sufficiently large, possesses an indefinite coefficient matrix A.

Often an approximation of the Sommerfeld radiation condition

$$\partial_r u - iku = o\left(r^{\frac{1-d}{2}}\right), \qquad r \to \infty,$$

where r is the radial variable, which specifies that wave motion should be outgoing on physically open boundaries, is imposed on part of the boundary. The Sommerfeld condition prescribes the asymptotic behavior of the solution, and its representation on finite boundaries leads to nonlocal operators. For this reason localized approximations of the Sommerfeld condition are used, the simplest of which is the Robin condition $\partial_n u - iku = 0$. As a result, the linear system (3) has a complex-symmetric, but non-Hermitian coefficient matrix as well as a complex-valued solution. The iterative solution of the discrete Helmholtz problem (3) is difficult, even for constant wave number k, and we will illustrate this in the first part of this paper, for Krylov methods, preconditioned Krylov methods, domain decomposition methods and multigrid. We then try to explain where these difficulties come from, and show what types of remedies have been developed over the last two decades in the literature. We will conclude the paper with some more recent ideas.

2 Problems of Classical Iterative Methods

2.1 Krylov Subspace Methods

Krylov subspace methods search for an approximate solution of the linear system (3) in the *Krylov space*

$$\mathscr{K}_m(A,\mathbf{f}) = \mathrm{span}\{\mathbf{f}, A\mathbf{f}, A^2\mathbf{f}, \ldots, A^{m-1}\mathbf{f}\} = \mathrm{span}\{\mathbf{q}_0, \mathbf{q}_1, \mathbf{q}_2, \ldots, \mathbf{q}_{m-1}\}, \tag{4}$$

where we have made the common choice of a zero initial guess for the solution, as is recommended in the absence of any additional information, see for example [50]. We show in Figure 1 how the wave number k fundamentally influences the solution of the Helmholtz equation. We have set homogeneous Dirichlet conditions on all boundaries, except on the left, where the Robin condition $\partial_n u - iku = 0$ was imposed, and used a point source in the corner. In the case of Laplace's equation ($k = 0$) the solution is large only near the point source in the corner, whereas for $k = 25$, the solution is large throughout the domain. The Krylov space constructed in (4), however, is very similar for both problems: due to the local connectivity

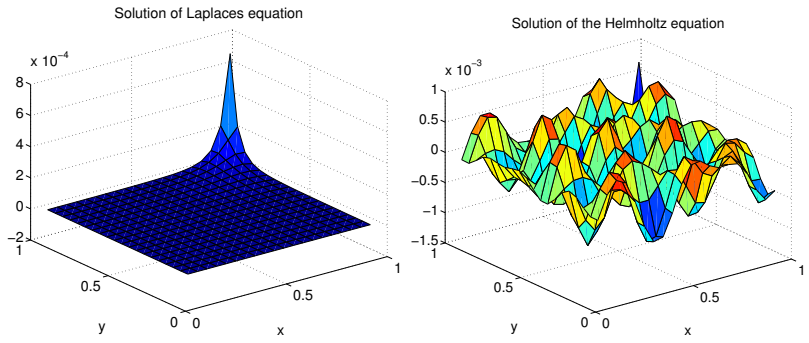

Fig. 1 Solution of Laplace's equation on the left, with a point source on the boundary, and on the right the solution of the Helmholtz equation, with the same boundary conditions.

(we used a five-point finite difference discretization for the Laplacian), the vector $\mathbf{f}$ is zero everywhere, except for the grid point connected to the boundary, and thus the Arnoldi vector $\mathbf{q}_0$ is just a canonical basis vector $(1,0,\ldots,0)^T$. The next vector in the Krylov space, $A\mathbf{f}$, is then non-zero only for the points connected with the first point, and the corresponding Arnoldi vector $\mathbf{q}_1$ will have only two non-zero entries, and so on. In the case of Laplace's equation we see that the first Arnoldi vectors are precisely non-zero where the solution is large, and thus it can be well approximated in the Krylov space. By contrast, in the indefinite Helmholtz case, where the solution is of the same size throughout the domain, these vectors do not have an appropriate support to approximate the solution. We show in Figure 2 how this influences the convergence of GMRES. While the residual decreases well in

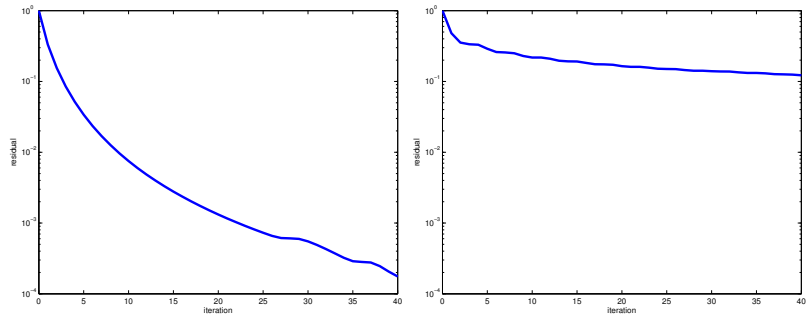

Fig. 2 Evolution of the residual for GMRES, on the left for the case of Laplace's equation, $k = 0$, and on the right for the Helmholtz equation, $k = 25$.

the Laplace case over the first $2 \times n$ iterations, where n is the number of grid points in one direction, convergence stagnates in the Helmholtz case. For a more precise quantitative analysis of this phenomenon, see [35]. Similar effects are also observed in the advection dominated case of advection diffusion equations, see [23, 50]. It

is therefore important to have a preconditioner, a Krylov method alone is not an effective iterative solver.

2.2 Algebraic Preconditioners Based on Factorization

The idea of preconditioning is as follows: instead of solving the original discretized system

$$A\mathbf{u} = \mathbf{f},$$

we solve the preconditioned system

$$M^{-1}A\mathbf{u} = M^{-1}\mathbf{f}, \tag{5}$$

where M is the so-called preconditioner. Preconditioners often arise from a stationary iterative method

$$M\mathbf{u}^{k+1} = N\mathbf{u}^k + \mathbf{f} \tag{6}$$

derived from a *matrix splitting* $A = M - N$ with M nonsingular. It is well known that this method converges asymptotically rapidly, if the spectral radius of the iteration matrix $M^{-1}N$ is small. This implies that the preconditioned matrix in (5),

$$M^{-1}A = M^{-1}(M-N) = I - M^{-1}N$$

has a spectrum clustered around 1 in the complex plane, which leads to fast asymptotic convergence also for a Krylov method applied to the preconditioned system (5). Clearly the best preconditioner would be A^{-1}, since this makes the spectral radius of $M^{-1}N$ vanish, since $M^{-1}N$=$A^{-1}0 = 0$, and all the eigenvalues of the preconditioned system $M^{-1}A = I$ equal 1. But then one could directly solve the system without iteration.

The idea of factorization preconditioners is to use an approximation of A^{-1} by computing an approximate LU factorization of the matrix A, $A \approx LU$, and then in each iteration step of (5), a forward and a backward substitution need to be performed. Two popular algebraic variants are the ILU(0) and ILU(tol) preconditioners, see [57]. For ILU(0), one computes an approximate LU factorization, keeping entries in the LU factors only if the corresponding entry in the underlying matrix A is non-zero. In the ILU(tol) variant, elements are kept, provided they are bigger than the tolerance tol. We compare in Table 1 the performance of this type of preconditioner when applied to the Helmholtz equation, for the case of growing wave number k. We solve an open cavity problem as in the previous example in Section 2.1, but now with a point source in the center. For this experiment, we keep the number of points per wavelength (more precisely, the ratio of wavelength to mesh spacing) constant, which means that the grid is refined with increasing wave number. We observe that the ILU preconditioners are quite effective for small wave numbers, but their performance deteriorates when k becomes larger: the situation with ILU('0') is worse than without preconditioning, and even ILU(tol) with a small drop tolerance

	QMR		ILU('0')		ILU(1e-2)	
k	it	Mflops	it	Mflops	it	Mflops
5	197	120.1	60	60.4	22	28.3
10	737	1858.2	370	1489.3	80	421.4
15	1775	10185.2	> 2000	> 18133.2	220	2615.1
20	> 2000	> 20335.1	—	—	> 2000	> 42320.1

Table 1 Iteration counts for QMR with and without preconditoner, applied to an indefinite Helmholtz equation with increasing wave number.

does not permit the solution of the problem. Similar results are also observed when using GMRES and other Krylov methods, see [36].

2.3 Domain Decomposition Methods

The oldest and simplest domain decomposition method is due to Schwarz [59]. He invented his alternating method in order to prove the Dirichlet principle, on which Riemann had based his theory of analytic functions of a complex variable (See [37] for a historical overview, and also [31] for an overview over the different continuous and discrete variants of the Schwarz method). The idea of the alternating Schwarz method is illustrated in Figure 3. One simply solves the original partial differential

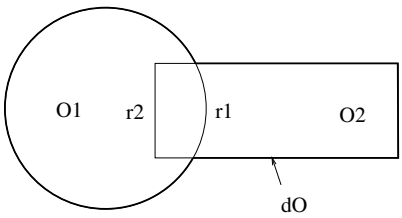

Fig. 3 Original drawing of a domain decomposition by Schwarz on the left, and on the right using the notation in the text

.

equation alternatingly in overlapping subdomains, and uses as interface condition the trace of the previously computed solution in the neighboring subdomain. For the case of the Helmholtz equation and the two subdomain decomposition in Figure 3, the algorithm is

$$\begin{aligned} -(\Delta + k^2)u_1^{n+1} &= 0 \quad \text{in } \Omega_1, & -(\Delta + k^2)u_2^{n+1} &= 0 \quad \text{in } \Omega_2, \\ u_1^{n+1} &= u_2^n \quad \text{on } \Gamma_1, & u_2^{n+1} &= u_1^{n+1} \quad \text{on } \Gamma_2. \end{aligned} \tag{7}$$

We show in Table 2 numerical experiments for growing wave number k for the case of a cavity open both on the left and on the right. We used the alternating

k	Overlap	10π	20π	40π	80π	160π
Iterative	h	div	div	div	div	div
Preconditioner	h	20	33	45	69	110
Iterative	fixed	div	div	div	div	div
Preconditioner	fixed	16	23	43	86	155

Table 2 Performance of a classical Schwarz domain decomposition method for a discretized Helmholtz equation

Schwarz method both as an iterative solver, as in (6), and as a preconditioner, as in (5), for GMRES. We see that the alternating Schwarz method is not convergent for the indefinite Helmholtz equation. Used as a preconditioner, we obtain a convergent method, but iteration numbers grow with increasing wave number k. For diffusive problems, the alternating Schwarz method converges better, if the overlap is increased, which is also intuitively understandable. This is, however, not the case for the Helmholtz equation, as we see comparing the case with overlap h, the mesh size, and with fixed overlap, equal to $2h$ on the coarsest grid, and then $4h$, $8h$ etc when the mesh is refined: at the beginning, for small wave numbers, overlap seems to help, but later, bigger overlap is detrimental to the performance of the Schwarz preconditioner when applied to the Helmholtz equation.

2.4 Fictitious Domain Methods

While domain decomposition methods arrive at more manageable subproblems by dividing a given problem region into smaller subregions, *fictitious domain methods* are based on imbedding the former in a larger domain for which a more efficient solver may be available. The first such techniques [44, 58, 11, 55], also known as *domain imbedding* or *capacitance matrix methods*, were developed to extend the efficiency of *fast Poisson solvers* based on the Fast Fourier Transform or cyclic reduction also to problems for which these methods are not directly applicable, as they require some form of separation of variables. In [21] (see also [22]) this idea was applied to exterior boundary value problems for the Helmholtz equation in two dimensions, and it was shown how the Sommerfeld radiation condition can be incorporated into a fast Poisson solver. Large-scale scattering calculations using this approach can be found in [43].

Computationally, fictitious-domain methods represent the original discrete problem as a low-rank modification of a larger problem amenable to fast methods. The fast solver plays the role of a discrete Green's function much in the same way its continuous counterpart is used in the integral equation method for solving the Helmholtz equation using layer potentials [13]. In fact, fictitious domain methods require the solution of an auxiliary system of equations which is a discretization of an integral operator on the boundary of the problem (scattering) domain. If a suitable formulation is chosen these operators are often compact perturbations of the

identity, which can be exploited to obtain mesh-independent convergence for iterative solution methods. The dependence on the wave number, however, is typically linear. Convergence independent of the wave number and mesh size would require more efficient preconditioning schemes for the discrete integral operator, which are currently not available. Recent developments on the spectral analysis of such operators necessary for the design of effective preconditioners can be found in [7].

2.5 Multigrid Methods

Two fundamental observations led to the invention of multigrid methods:

- When applied to the Poisson equation, classical stationary iterative methods such as Gauss-Seidel or damped Jacobi iteration effectively remove high-frequency components of the error, but are very ineffective for low-frequency components. Stiefel points this out very vividly in his 1952 paper [61] on precursors of the conjugate gradient method, remarking that, after a few iterations of one of such basic iterative methods, in which the residual is reduced significantly, subsequent iteration steps decrease the residual only by very little, as if the approximation were confined to a "cage" [1].
- The remaining low-frequency components in the error can be well represented on a coarser grid,[2] as Federenko points out in his 1961 paper presenting the first complete multigrid method [28]:

> We shall speak of the eigenfunctions as "good" and "bad"; the good ones include those that are smooth on the net and have few changes of sign in the domain; the bad ones often change sign and oscillate rapidly [...] After a fairly small number of iterations, the error will consist of "good" eigenfunctions [...] We shall use the following method to annihilate the "good" components of the error. We introduce into the domain an auxiliary net, the step of which is q times greater than the step of the original net.

The simplest multigrid scheme to which these developments led is the classical 'V-cycle', which, applied to the system $A\mathbf{u} = \mathbf{f}$, reads:

[1] "Das Auftreten von Käfigen ist eine allgemeine Erscheinung bei Relaxationsverfahren und sehr unerwünscht. Es bewirkt, dass eine Relaxation am Anfang flott vorwärts geht, aber dann immer weniger ausgiebig wird . . . "

[2] The idea of beginning the iteration on a coarse grid with a subsequent "advance to a finer net", not unlike the modern *full multigrid* approach, was in use already in the early days of "relaxation methods", as evidenced, e.g., in the book of Southwell [60, Section 52] from 1946.

```
function u=Multigrid(A,f,u0);
if isSmall(A) then u=A\f else
      u=DampedJacobi(nu,A,f,u0);
      r=Restrict(f-Au);
      e=Multigrid(Ac,r,0);
      u=u+Extend(e);
      u=DampedJacobi(nu,A,f,u);
end;
```

We show in Table 3 the performance of the multigrid algorithm when applied to a discretized Helmholtz equation, in our example a closed cavity without resonance for the discretized problem[3]. We observe that the multigrid method is not converging

k	Smoothing steps	2.5π	5π	10π	20π
Iterative	$\nu = 2$	7	div	div	div
Preconditioner	$\nu = 2$	6	12	41	127
Iterative	$\nu = 5$	7	stag	div	div
Preconditioner	$\nu = 5$	5	13	41	223
Iterative	$\nu = 10$	8	div	div	div
Preconditioner	$\nu = 10$	5	10	14	87

Table 3 Performance of a classical geometric multigrid method with optimally damped Jacobi smoother applied to a discretized Helmholtz equation

as an iterative solver except for a very small wave number. When multigrid is used as a preconditioner, we obtain a convergent method, like in the case of the Schwarz domain decomposition method, but again the iteration numbers grow substantially when the wave number increases. We used again about 10 points per wavelength in these experiments. Often one increases the number of smoothing steps in the multigrid method, to improve the performance, and we see in Table 3 that for small wave numbers, this seems to help the preconditioned version, but for large wave numbers, adding more smoothing steps can both increase and decrease performance. Again, we observe that the Helmholtz operator is not suitable to be solved with standard multigrid.

[3] In a closed cavity, i.e., with homogeneous Dirichlet conditions imposed on all sides, it is important to ensure that k^2 is not an eigenvalue of the *discrete* Laplacian, since otherwise one obtains a singular matrix. In the case of a multigrid solver then, one must be careful that k^2 is not an eigenvalue of the discrete Laplacian on each of the grids used in the multigrid hierarchy, which we did for this experiment (see also subsection 3.4)

3 Iterative Methods for Helmholtz Problems

We now describe several iterative methods and preconditioners which have been developed especially for solving discrete Helmholtz problems. In each case we first give an explanation of why the classical iterative method or preconditioner fails, and then show possible remedies.

3.1 Analytic Incomplete LU

The incomplete LU (ILU) preconditioners are based on the fact that the linear system (3) could be solved by a direct factorization, the so called LU factorization

$$A = LU, \qquad L \text{ lower triangular}, \quad U \text{ upper triangular}. \tag{8}$$

The solution of the linear system $A\mathbf{u} = LU\mathbf{u} = \mathbf{f}$ is then obtained by solving

$$\begin{aligned} L\mathbf{v} &= \mathbf{f} \quad \text{by forward substitution,} \\ U\mathbf{u} &= \mathbf{v} \quad \text{by backward substitution.} \end{aligned}$$

If the matrix A is a discretization of the Helmholtz operator $-(\Delta + k^2)$ in two dimensions, and we use the lexicographic ordering of the unknowns indicated in Figure 4, we can interpret the forward and backward substitutions geometrically: the forward

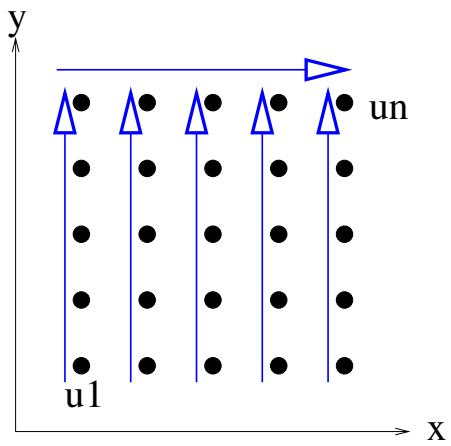

Fig. 4 Ordering of the unknowns in the discretization of the Helmholtz operator

substitution process $L\mathbf{v} = \mathbf{f}$ determines first the variables in the leftmost column of the domain, see Figure 4, then in the second leftmost, and so on, until the last column on the right. The process is sequential, and could be interpreted as a time-stepping

in the positive x-direction, solving some type of evolution problem. The backward substitution process $U\mathbf{u} = \mathbf{v}$, on the other hand, starts with the variables in the rightmost column in Figure 4, and then computes the second rightmost column, and so on, until the first column on the left is determined. Again the process is sequential, and could be interpreted as a time-stepping, but this time in the negative x-direction.

From the explanation of the convergence of Krylov methods without preconditioning given in Section 2, we see that efficient transport of information in the preconditioner is important for Helmholtz problems. We have, however, also seen that the classical ILU preconditioners do not seem to bring about this transport effectively enough: even the quite accurate approximate ILU(1e-2) factorization does not suffice.

In order to find what the evolution problems described by the LU factorization could correspond to for the underlying Helmholtz equation, we looked in [36] for a factorization of the Helmholtz operator in the x direction,

$$-(\Delta + k^2) = -(\partial_x + \Lambda_1)(\partial_x - \Lambda_2), \tag{9}$$

where Λ_1 and Λ_2 are (non-local) operators to be determined such that the factorization in (9) holds. If we have such a factorization at the continuous level, then we can solve $-(\Delta + k^2)u = -(\partial_x + \Lambda_1)(\partial_x - \Lambda_2)u = f$ by solving two evolution problems:

$$\begin{aligned} -(\partial_x + \Lambda_1)v &= f \quad \text{evolution problem in the forward } x \text{ direction,} \\ (\partial_x - \Lambda_2)u &= v \quad \text{evolution problem in the backward } x \text{ direction.} \end{aligned}$$

Taking a Fourier transform in the y-direction with Fourier variable ξ, we obtain

$$\mathscr{F}_y(-(\Delta + k^2)) = -\partial_{xx} + \xi^2 - k^2 = -(\partial_x + \sqrt{\xi^2 - k^2})(\partial_x - \sqrt{\xi^2 - k^2}), \tag{10}$$

and thus we have the continuous analytic factorization of the Helmholtz operator

$$-(\Delta + k^2) = -(\partial_x + \Lambda_1)(\partial_x - \Lambda_2), \tag{11}$$

where $\Lambda_1 = \Lambda_2 = \mathscr{F}_y^{-1}(\sqrt{\xi^2 - k^2})$. Note that the Λ_j, $j = 1,2$, are non local operators in y, because of the square root in their symbol $\sqrt{\xi^2 - k^2}$.

The discrete analog of this factorization at the continuous level is the block LDL^T factorization of the discrete Helmholtz matrix A. In the case of a five point finite difference discretization, this matrix has the block structure

$$A = \frac{1}{h^2}\begin{bmatrix} A_1 & -I & \\ -I & A_2 & \ddots \\ & \ddots & \ddots \end{bmatrix}, \quad A_j = \begin{bmatrix} 4-kh^2 & -1 & \\ -1 & 4-kh^2 & \ddots \\ & \ddots & \ddots \end{bmatrix}.$$

A direct calculation shows that the block LDL^T factorization of A is given by

$$L = \frac{1}{h}\begin{bmatrix} I & & & \\ -T_1^{-1} & I & & \\ & -T_2^{-1} & \ddots & \\ & & \ddots & \ddots \end{bmatrix}, \quad D = \begin{bmatrix} T_1 & & \\ & T_2 & \\ & & \ddots \end{bmatrix},$$

where the matrices T_j satisfy the recurrence relation

$$T_{j+1} = A_{j+1} - T_j^{-1}, \quad T_1 = A_1, \tag{12}$$

it suffices to multiply the matrices in order to verify. We observe that in this exact factorization, the matrices T_j are no longer sparse, since the recurrence relation (12) which determines them involves an inverse. This fill in at the discrete level corresponds to the non-local nature of the operators Λ_j. Using a local approximation of the matrices T_j with tridiagonal structure only gives an approximate LDL^T factorization of A which we call AILU('0') (Analytic Incomplete LU). In order to obtain a good approximation, the relation to the continuous factorization was used in [36], and the spectral radius of the corresponding iteration matrix was minimized. The performance of this preconditioner, which is now tuned for the Helmholtz nature of the problem, is shown in Table 4, for the same open cavity problem as before. We

	QMR		ILU('0')		ILU(1e-2)		AILU('0')	
k	it	Mflops	it	Mflops	it	Mflops	it	Mflops
5	197	120.1	60	60.4	22	28.3	23	28.3
10	737	1858.2	370	1489.3	80	421.4	36	176.2
15	1775	10185.2	2000	18133.2	220	2615.1	43	475.9
20	2000	20335.1	—	—	2000	42320.1	64	1260.2
30	–	–	–	–	–	–	90	3984.1
40	–	–	–	–	–	–	135	10625.0
50	–	–	–	–	–	–	285	24000.4

Table 4 Performance comparison of the specialized AILU('0') preconditioner, compared to the other ILU variants

clearly see that this approximate factorization contains much more of the physics of the underlying Helmholtz equation, and leads to a better preconditioner. Nevertheless, the iteration number is still growing with growing wave number k.

The AILU preconditioner goes back to the analytic factorization idea, see [53] and references therein. It is very much related to the Frequency Filtering Decomposition, as proposed by Wittum in [64, 65] and analyzed for symmetric positive problems in [62], and for non-symmetric problems in [63]. There was substantial research activity for these kinds for preconditioners around the turn of the century, see [40], [12], [29], [1], and for Helmholtz problems this is one of the best incomplete factorization preconditioners available. For more recent work, see [2], [54], and for Helmholtz problems in particular [18] and [19], where this type of preconditioner is called a 'sweeping preconditioner', and an optimal approximation is proposed in the sense that iteration numbers do not depend on the wave number k any more.

3.2 Domain Decomposition Methods for Helmholtz Problems

In the late 1980s researchers realized that classical domain decomposition methods were not effective for Helmholtz problems, and the search for specialized methods began. In his PhD thesis [15], Bruno Després summarizes this situation precisely:

> L'objectif de ce travail est, après construction d'une méthode de décomposition de domaine adaptée au problème de Helmholtz, d'en démontrer la convergence[4].

The fundamental new ingredient for such an algorithm turned out to be the transmission condition between subdomains, as in the non-overlapping variant of the Schwarz algorithm proposed by Lions [51]. The algorithm proposed by Bruno Després is

$$\begin{aligned} -(\Delta + k^2)u_j^{n+1} &= f, && \text{in } \Omega_j \\ (\partial_{n_j} - ik)u_j^{n+1} &= (\partial_{n_j} - ik)u_l^n, && \text{on interface } \Gamma_{jl}, \end{aligned} \tag{13}$$

and, on comparing with the classical alternating Schwarz algorithm in (7), we see that now a Robin transmission condition is used at the interfaces. The algorithm was considered by Després for many subdomains, but only without overlap, so that its convergence can be proved using energy estimates.

In order to get more insight why the transmission conditions are important, we show in Figure 5 the convergence factor of the algorithm for the simple model problem of a square decomposed into two rectangles. In this case, we can use Fourier series in the direction of the interface to explicitly compute how each Fourier mode converges, see for example [34]. We see on the left for the classical alternating

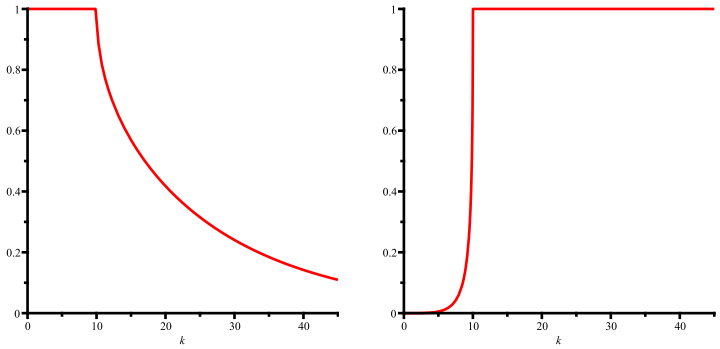

Fig. 5 Comparison of how each Fourier mode in the error converges, on the left for the classical alternating Schwarz method with overlap, and on the right for the variant designed for the Helmholtz equation, without overlap

Schwarz method that low frequency modes are not converging at all, their conver-

[4] The goal of this work is to design a special domain decomposition method for Helmholtz problems, and to prove that it converges

gence factor equals one. These modes correspond to the oscillatory, or propagating modes in the solution of the Helmholtz equation, as are clearly visible, e.g., in the example in Figure 1 on the right. High-frequency components, however, converge well in the classical alternating Schwarz method. These modes correspond to evanescent modes, usually only well visible for diffusive problems, as in Figure 1 on the left. The situation for the non-overlapping method of Després on the right is reversed: the new transmission conditions lead to a rapidly converging method for the propagating modes in the low-frequency part of the spectrum, but now high frequency components are not converging.

Després wanted to prove convergence of the algorithm, and the technique of energy estimates generally works only for the non-overlapping variants of the algorithm. But Figure 5 suggests that one could use the overlap for the high-frequency modes, and the transmission condition for the low-frequency modes, in order to obtain a method effective for all modes in a Helmholtz problem. In addition, it might be possible to choose an even better transmission condition, as indicated toward the end in Lions' work [51], and also by Hagström et al. in [42]. All these observations and further developments led at the turn of the century to the invention of the new class of optimized Schwarz methods [33], with specialized variants for Helmholtz problems [34, 32]. For an overview for symmetric coercive problems, see [30].

Using optimized transmission conditions of zeroth order, which means choosing the best complex constant instead of ik in the Robin condition, we obtain for the same model problem as in Figure 5 the contraction factors shown in Figure 6 on the left. We can see that all modes, except for the resonance mode, now converge

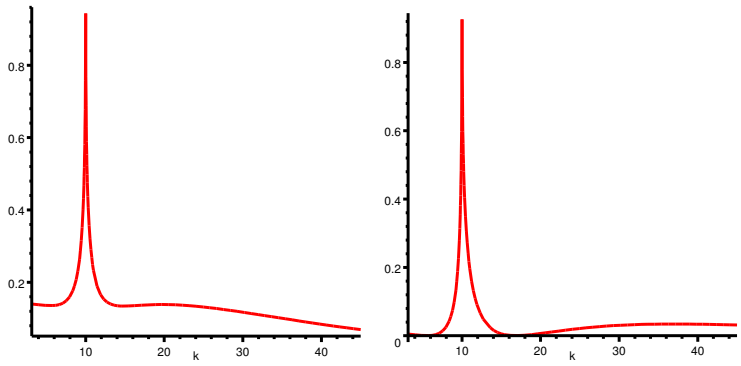

Fig. 6 Comparison of how each Fourier mode in the error converges, on the left for an optimized Schwarz method of order zero (OO0), and on the right for a second order optimized Schwarz method (OO2), both with overlap

well. On the right in the same figure, we show a second-order optimized Schwarz method, in which one also uses the Laplace-Beltrami operator at the interface to obtain an even more effective transmission condition. Using this operator does in no way increases the sparsity pattern of the subdomain solver, since second order derivatives are already present in the underlying discretization of the Laplacian.

A general convergence analysis of optimized Schwarz methods for Helmholtz problems currently only exists for the non-overlapping case, using energy estimates. This approach however does not allow us to obtain convergence factor estimates. In addition, to prove convergence for the general overlapping case is an open problem. For the model situation of two subdomains however, one can quantify precisely the dependence of the convergence factor on the wave number k, and the mesh parameter h. We show in Table 5 the resulting convergence factors from [32]. We

	k fixed	$k^\gamma h$ const
Overlap 0	$1-O(h^{\frac{1}{4}})$	$1-O(k^{\frac{1-2\gamma}{8}})$
Overlap $C_L h$	$1-O(h^{\frac{1}{5}})$	$\begin{cases} 1-O(k^{-\frac{1}{8}}) & 1 \le \gamma \le \frac{9}{8} \\ 1-O(k^{\frac{1-2\gamma}{10}}) & \gamma > \frac{9}{8} \end{cases}$
Overlap const	$1-const$	$1-O(k^{-\frac{1}{8}})$

Table 5 Asymptotic convergence factors obtained for a model problem

see that for a fixed wave number k, and a constant overlap, independent of the mesh size h, the algorithm converges with a contraction factor independent of the mesh size h. In the important case where the wave number k scales with the mesh size h like $k^\gamma h$ in order to avoid the pollution effect, see [45, 46], we see that the contraction factor only depends very weakly on the growing wave number: for example if the overlap is held constant, all Fourier modes of the error contract at least with a factor $1-O(k^{-\frac{1}{8}})$.

In Table 6, we show a numerical experiment for a square cavity open on two sides, and the non-overlapping optimized Schwarz method in order to illustrate the asymptotic results from Table 5. We used a fixed wave number k on the left, and a growing wave number k on the right, while again keeping ten points per wavelength. We show in the leftmost column the iterative version of the algorithm, in order to

	Iterative	Krylov			Krylov	
h	Optimized	Deprés	Optimized	k	Deprés	Optimized
1/50	322	26	14	10π	24	13
1/100	70	34	17	20π	33	18
1/200	75	44	20	40π	43	20
1/400	91	57	23	80π	53	21
1/800	112	72	27	160π	83	32

Table 6 Numerical experiment for a two-subdomain decomposition

illustrate the sensitivity of the algorithm with respect to the peak of the convergence factor at the resonance frequency. Since the discretization modifies the continuous spectrum, a discretization with insufficient resolution may have eigenvalues close to the resonance frequency, which are not taken into account by the continuous optimization based on Fourier analysis, which in turn can result in an arbitrarily large iteration count, as we see for example for $h = \frac{1}{50}$. Such problems, however,

disappear once the mesh is fine enough, or when Krylov acceleration is added, as one can observe in Table 6. This issue is therefore not of practical concern. We also see that it clearly pays to use optimized parameters, as the iteration count is substantially lower than with the first choice of ik in the transmission conditions.

We finally show two numerical experiments from [34] and [32], in order to illustrate that optimized Schwarz methods for Helmholtz equations also work well in more practical situations. In Figure 7, we simulated the approach of an Airbus A340

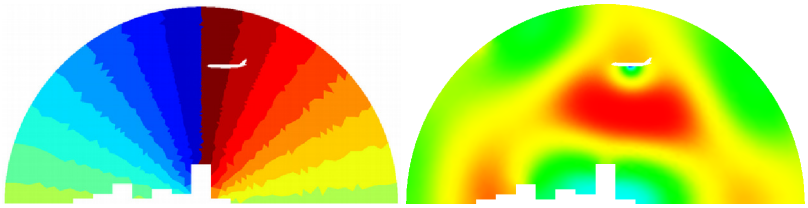

Fig. 7 Airbus A340 in approach over a city

over the silhouette of a city, with a decomposition into 16 subdomains. In this case, using a Robin transmission condition with ik as parameter required 172 iterations, whereas the optimized Schwarz method needed only 58 iterations to converge to the same tolerance. The second example is the interior of a Twingo car from Renault, shown in Figure 8. Here, the Robin transmission condition with ik as parameter took

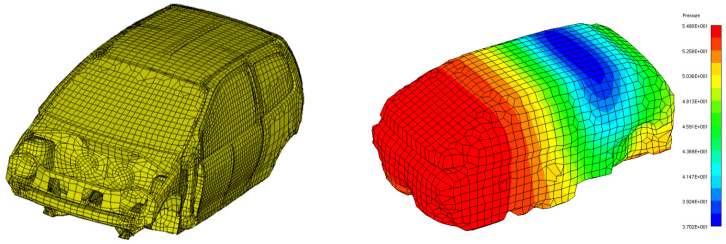

Fig. 8 Simulation of the noise in the passenger cabin of a Twingo car from Renault

105 iterations, and the optimized Schwarz method 34.

There is a second type of domain decomposition methods for Helmholtz problems, from the FETI class of methods (Finite Element Tearing and Interconnect, see [27]). These methods are based on a dual Schur complement formulation, which means that interior variables in the subdomains are eliminated, assuming that Neumann traces are continuous across interfaces, and then a substructured system is obtained by requiring that Dirichlet traces along interfaces match. A primal Schur formulation would do the opposite: eliminate interior unknowns of subomains, assuming that Dirichlet traces are continuous across interfaces, and then impose con-

tinuity of the Neumann traces along interfaces in order to obtain a substructured formulation. These methods usually need an additional preconditioner, in order to obtain convergence rates independent (or only weakly dependent) on the mesh parameter h. An optimal choice is to use the primal Schur complement method for the dual Schur complement formulation, and vice versa. In order to scale with the number of subdomains, also a coarse grid is needed. For the case of Laplace's equation, the classical coarse grid is to use a constant per subdomain, since if FETI is used to solve Laplace's equation, interior subdomain problems containing Neumann conditions all around have precisely the constant as a kernel. This idea transformed an inconvenience of the original FETI idea, namely that interior subdomains are singular, into a benefit: a natural coarse grid.

In order to adapt this class of methods to Helmholtz problems, the first variant was the FETI-H method (for FETI-Helmholtz), see [26]. Instead of using Neumann transmission conditions in the dual Schur complement formulation, Robin conditions $\partial_n - ik$ are used, but then still Dirichlet traces are matched in order to obtain a substructured formulation. This approach is thus very much related to an optimized Schwarz method without overlap; however, only one type of Robin conditions can be imposed, since the other one is Dirichlet. This means that always on one side of the interface, a Robin condition with the good sign is used, whereas on the other side, a Robin condition with the bad sign is imposed. For checkerboard type partitions, one can ensure that subdomains have only Robin conditions with constant sign all around. Otherwise, an algorithm was proposed to generate a choice of sign which guarantees that subdomain problems are not singular. The original formulation has no additional preconditioner, but a coarse grid in form of plane waves.

The second algorithm in the FETI class specialized for Helmholtz problems is FETI-DPH, see [24]. This is a FETI-DP formulation, which means that some interface unknowns are kept as primal variables, where continuity is enforced, and which serve at the same time as coarse space components. These are usually cross points, and in FETI-DPH additional primal constraints are enforced at the interfaces, using planar waves. Furthermore, a Dirichlet preconditioner is used on top, like in the classical FETI formulation. A convergence analysis exists for this algorithm, see [25], but it needs the assumption that subdomains are small enough. A systematic comparison of all currently existing domain decomposition algorithms for Helmholtz problems is in preparation, see [38].

3.3 Multigrid for Helmholtz Problems

We will see in this section that neither of the two fundamental observations made by Stiefel and Federenko, see Section 2, hold for the case of the Helmholtz equation. In an early theoretical paper about multigrid methods [5], Bakhvalov first advertises the method also for indefinite problems:

> For instance it is used in the case of the equation $\Delta u + \lambda u = f$ with large positive $\lambda(x_1, x_2)$. Previously no methods of solving this equation with good asymptotics for the number of operations were known

but then later in the paper he discovers potential problems:

> In the case of the equation $\Delta u + \lambda u = f$ with large positive λ we do not exclude the possibility that the evaluation of (3.21) may be attained in order. Then the increase in the number m in comparison with that calculated can lead to a deterioration in the discrepancy of the approximation.

It took more than three decades, before Brandt and Livshits [9] took on the difficult Helmholtz case again, and they try to explain the origin of the difficulties of the multigrid algorithm:

> On the fine grids, where [the characteristic components] are accurately approximated by the discrete equations, they are invisible to any local relaxation, since their errors can have very small residuals. On the other hand, on coarser grids such components cannot be approximated, because the grid does not resolve their oscillations.

Similarly, Lee, Manteuffel, McCormick and Ruge [4] explain the problem as follows:

> Helmholtz problems tax multigrid methods by admitting certain highly oscillatory error components that yield relatively small residuals. Because these components are oscillatory, standard coarse grids cannot represent them well, so coarsening cannot eliminate them effectively. Because they yield small residuals, standard relaxation methods cannot effectively reduce them.

In order to more precisely illustrate the problems of the multigrid algorithm when applied to the Helmholtz equation, we consider now the Helmholtz equation in two dimensions on the unit square,

$$-(\Delta + k^2)u = f, \quad \text{in } \Omega := (0,1) \times (0,1). \tag{14}$$

We show two numerical experiments, following the strategy of Boris Diskin [16], that in order to investigate the behavior of multigrid methods, one should replace one of the two components (smoother or coarse grid correction) by a component which one knows to be effective (even if it is not feasible to use this component in practice), to test the other one. In a first experiment, we use a Fourier smoother in order to remove explicitly the high frequency components of the error, and try to compute the solution shown in Figure 9, in the top left graph, which corresponds to the choice of parameters $f = -\frac{1}{20}$, $k^2 = 19.7$ and fine grid parameter $h = \frac{1}{32}$. We use a random initial guess u_0, and a two grid cycle. The result is shown in Figure 9.

We clearly observe the following in this experiment: while the error on the coarse grid is well resolved, the correction calculated on the coarse grid is 100% incorrect, it has the wrong sign! Hence the problem does not seem to be that certain high frequency components in the error are left to the coarse grid and cannot be approximated accurately there: the mesh is largely fine enough to represent them. But the correction calculated is incorrect: it is the operator itself which is not well approximated. This had already been discovered in an earlier paper by Brandt and Ta'asan [8] on slightly indefinite problems:

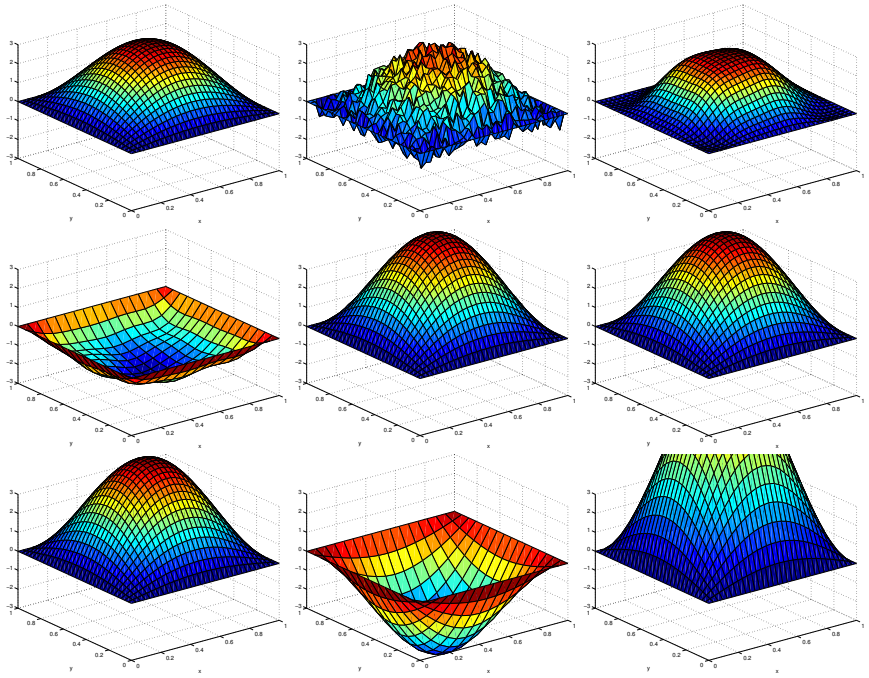

Fig. 9 Problem of the coarse grid correction when multigrid is used for the Helmholtz equation. From top left to bottom right: solution we want to calculate, and then initial error, error after presmoothing, coarse grid correction that needs to be *subtracted*, error after coarse grid correction, error after postsmoothing, error after presmoothing, coarse grid correction that needs to be *subtracted*, error before postsmoothing.

Usual multigrid for indefinite problems is sometimes found to be very inefficient. A strong limitation exists on the coarsest grid to be used in the process. The limitation is not so much a result of the indefiniteness itself, but of the nearness to singularity, that is, the existence of nearly zero eigenvalues. These eigenvalues are badly approximated (e.g. they may even have a different sign) on coarse grids, hence the corresponding eigenfunctions, which are usually smooth ones, cannot efficiently converge.

For our second numerical experiment, we now use a damped Jacobi smoother, and compute the exact coarse grid correction, by computing it on the fine grid, then restricting it to the coarse grid and prolongating it again to the fine grid, in order to guarantee that the coarse grid correction is working properly (this would not make sense obviously in a real multigrid code, but allows us to illustrate the reason why the smoother fails). We try to compute the solution shown in Figure 10, in the top left graph, which corresponds to the parameters $f = -1000$, $k^2 = 400$ and fine mesh size $h = \frac{1}{32}$, and we use again a random initial guess u_0, and a two grid cycle. Its behavior is shown in Figure 10 in the remaining graphs. We clearly see that even though the coarse grid correction is very effective, the smoother is responsible for a growing low frequency mode, and the two grid method does not converge. We explain these two observation in the next section with a detailed two-grid analysis.

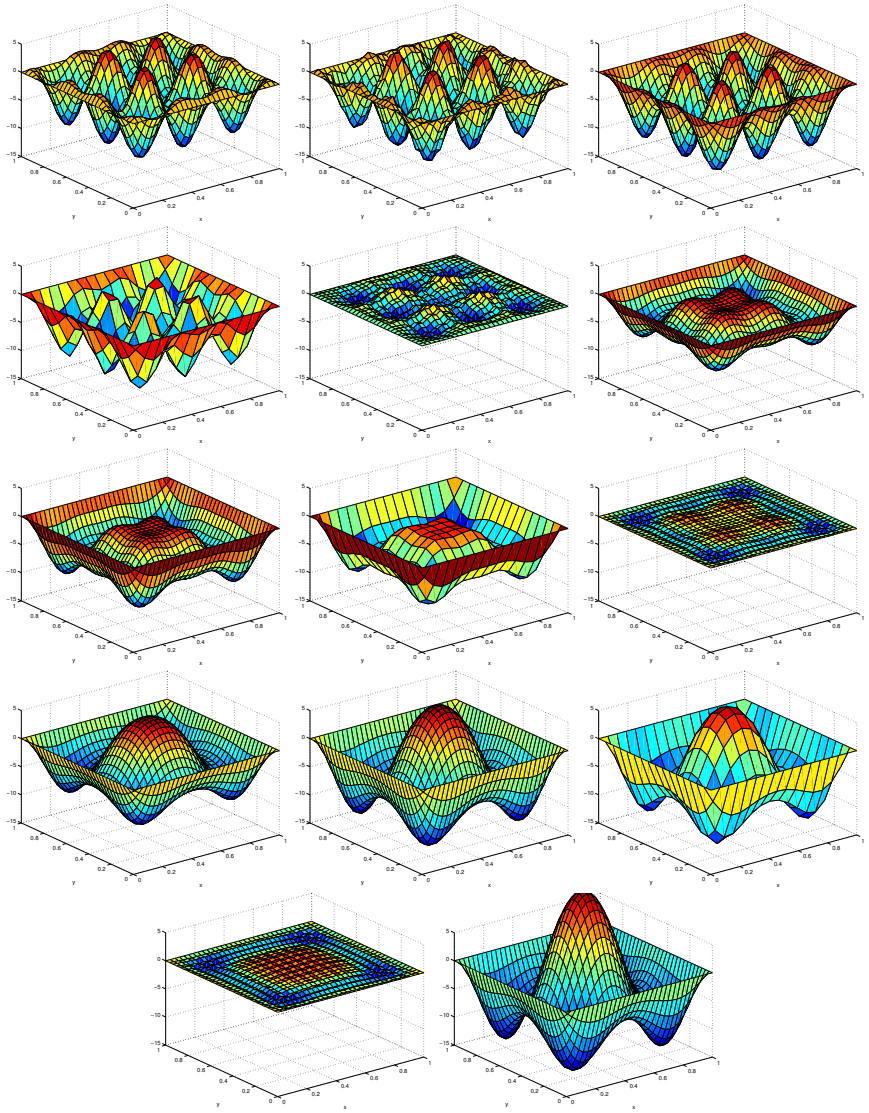

Fig. 10 Problem of the smoother when multigrid is used for the Helmholtz equation. From top left to bottom right: solution we want to calculate, and then initial error, error after presmoothing, coarse grid correction that needs to be *subtracted*, error after coarse grid correction, error after postsmoothing, error after presmoothing, coarse grid correction that needs to be *subtracted*, error before postsmoothing, etc

3.4 Two-Grid Analysis for the 1D Model Problem

To explain the difficulties of multigrid applied to the Helmholtz equation, we consider the simplest possible case of the one-dimensional problem

$$-u'' - k^2 u = f \quad \text{in } \Omega = (0,1), \qquad u(0) = u(1) = 0, \tag{15}$$

with constant wave number k and peform a spectral analysis, much along the lines of [41, Chapter 2] and [10, Chapter 5].

We assume that k^2 is not an eigenvalue of the Dirichlet-Laplacian for this domain and therefore the continuous problem possesses a unique solution, as do sufficiently accurate discrete approximations. When multigrid is applied to cavity problems like (15) one must always be careful that all coarse-grid problems are nonsingular. This is, however, no longer an issue when damping is present, either in the form of an absorbing medium or radiation boundary conditions.

Using the standard three-point centered finite-difference approximation of the second derivative on a uniform mesh with N interior grid points and mesh width $h = 1/(N+1)$, (15) is approximated by the linear system of equations $\mathbf{Au} = \mathbf{f}$ for the function values $u(x_j) \approx u_j, j = 1,\ldots,N$, at the grid points $x_j = jh$, where

$$\mathbf{A} = \frac{1}{h^2}\,\text{tridiag}(-1, 2-k^2h^2, -1) \in \mathbb{R}^{N\times N}. \tag{16}$$

The matrix $\mathbf{A}$ is symmetric and has the complete set of orthogonal eigenvectors

$$\mathbf{v}_j = [\sin j\ell\pi h]_{\ell=1}^{N}, \qquad j = 1,\ldots,N. \tag{17}$$

When it is necessary to rescale these eigenvectors to have unit Euclidean norm this is achieved by the factor $\sqrt{2h}$ (for all j). The associated eigenvalues are given by

$$\lambda_j = \frac{2(1-\cos j\pi h)}{h^2} - k^2 = \frac{4}{h^2}\sin^2\frac{j\pi h}{2} - k^2, \qquad j = 1,\ldots,N.$$

The form of the eigenvectors (17) reveals that these become more oscillatory with increasing index j.

When N is odd, which we shall always assume for the pure Dirichlet problem, we set $n := (N-1)/2$ and refer to the eigenpairs associated with the indices $1 \le j \le n$ as the *smooth* part of the spectrum I_{sm} and the remainder as the *oscillatory* part I_{osc}. Note that the eigenvalue with index $j = (N+1)/2 = n+1$ lies exactly in the middle, with an associated eigenvector with wavelength $4h$.

3.4.1 Smoothing

The Jacobi smoother is based on the splitting $A = D - (D-A)$ of the matrix A in (16), where $D = \text{diag}(A)$, resulting in the iteration

$$\mathbf{u}_{m+1} = \mathbf{u}_m + D^{-1}(\mathbf{f} - A\mathbf{u}_m).$$

For smoothing one usually introduces a damping factor ω for the update, giving

$$\mathbf{u}_{m+1} = \mathbf{u}_m + \omega D^{-1}(\mathbf{f} - A\mathbf{u}_m), \tag{18}$$

which corresponds to the splitting $A = \frac{1}{\omega}D - (\frac{1}{\omega}D - A)$. The associated error propagation operator is

$$S_\omega = I - \omega D^{-1}A. \tag{19}$$

Noting that $D = (2/h^2 - k^2)I$, we conclude that A and D are simultaneously diagonalizable, which gives for S_ω the eigenvalues

$$\sigma_j = \sigma_j(\omega) = 1 - \omega\left(1 - \frac{2\cos j\pi h}{2 - k^2h^2}\right) =: 1 - \omega\frac{\lambda_j}{\delta}, \qquad j = 1,\ldots,N, \tag{20}$$

where we have introduced $\delta = \delta(k,h) := (2 - k^2h^2)/h^2$ to denote the diagonal entry in the Jacobi splitting, which is constant for this model problem.

In multigrid methods the smoothing parameter ω is chosen to maximize damping on the oscillatory half of the spectrum I_{osc}. For the Laplace operator ($k = 0$) the eigenvalues of $D^{-1}A$ are given by $\lambda_j/\delta = 1 - \cos(j\pi h)$, $j = 1,\ldots,N$, resulting in, up to order h^2, the spectral interval $[0,2]$, with $I_{\text{osc}} = [1,2]$. Maximal damping on $I_{\text{osc}} = [1,2]$ thus translates to the requirement of equioscillation, i.e.,

$$1 - \omega = -(1 - 2\omega), \qquad \text{i.e.} \qquad \omega = \omega_0 := \frac{2}{3}. \tag{21}$$

For this optimal value of the damping parameter ω each eigenmode belonging to the oscillatory modes $\text{span}\{\mathbf{v}^h_{n+1},\ldots,\mathbf{v}^h_N\}$ is reduced by at least a factor of

$$\sigma_{n+1}(\omega_0) = 1 - \omega_0 = \frac{1}{3}$$

in each smoothing step, independently of the mesh size h. Figure 11 shows the spectrum of S_ω for the discrete 1D Laplacian on the unit interval with mesh width $h = 1/50$ for the values $\omega = 0$ (undamped) and the optimal value $\omega = 2/3$, plotted against the eigenvalues λ_j of A.

For the 1D Helmholtz operator ($k > 0$) the eigenvalues of $D^{-1}A$ are

$$\frac{\lambda_j}{\delta} = 1 - \frac{2\cos j\pi h}{2 - k^2h^2}, \qquad j = 1,\ldots,N,$$

and therefore, up to $O(h^2)$, these range between the extremal values

$$\frac{\lambda_1}{\delta} = \frac{-k^2h^2}{2 - k^2h^2}, \qquad \text{and} \qquad \frac{\lambda_N}{\delta} = \frac{4 - k^2h^2}{2 - k^2h^2}.$$

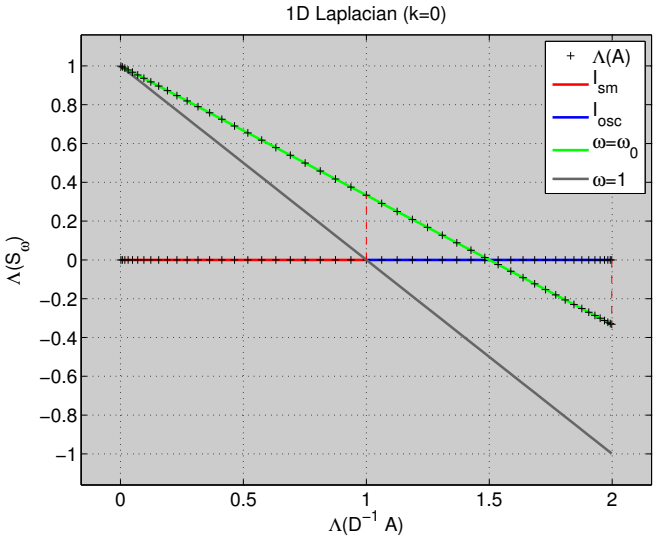

Fig. 11 Eigenvalues of the undamped and optimally damped Jacobi smoother plotted against those of the associated diagonally scaled 1D Laplacian $-\Delta_h$, $h = 1/50$, divided into smooth and oscillatory parts I_{sm} and I_{osc}. The dashed red lines indicate the spectral radius of S_ω restricted to the space of oscillatory eigenfunctions.

Assuming the midpoint $(\lambda_1 + \lambda_N)/2$ is still positive, maximal smoothing of the oscillatory modes can again be obtained by equioscillation, which fixes ω by requiring

$$1 - \omega\frac{\lambda_N}{\delta} = -\left(1 - \omega\frac{\lambda_1 + \lambda_N}{2\delta}\right),$$

and gives

$$\omega = \omega_k := \frac{2 - k^2h^2}{3 - k^2h^2}. \tag{22}$$

Figure 12 shows the analogous quantities of Figure 11 for the Helmholtz equation with wave number $k = 10\pi$. In contrast with the Laplacian case, the spectrum of A now extends into the negative real axis. By consequence, any choice of the relaxation parameter ω will result in amplification of some modes, as we have seen in our example in Figure 10. In the case shown, these are precisely the eigenmodes of A associated with negative eigenvalues. If this only constitutes a small portion of $\Lambda(A)$, then the coarse grid correction, the second component of multigrid methods which eliminates smooth error components, can be expected to compensate for this amplification. It is clear, however, that the amplification will both grow too large and extend over too large a portion of the spectrum for smaller and smaller wave resolution, i.e., kh large.

Therefore, fundamentally different smoothing iterations are needed for Helmholtz problems. For this reason Brandt and T'asan [8] proposed using the Kazmarcz re-

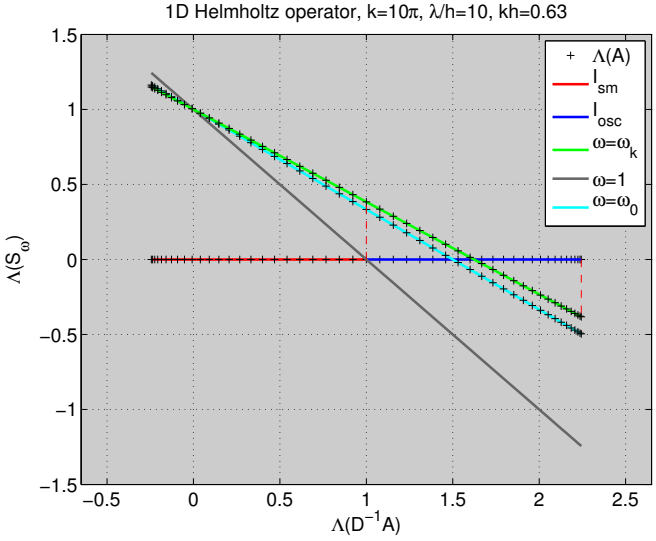

Fig. 12 Eigenvalues of the Jacobi smoother plotted with $\omega = \omega_k$, $\omega = \omega_1$ and $\omega = \omega_0$ against those of the associated diagonally scaled 1D Helmholtz operator $-\Delta_h - k^2$, $h = 1/50$ with wavelength-to-mesh ratio $\lambda/h = 10$.

laxation, which is essentially Gauss-Seidel iteration applied to the normal equations. This smoother has the advantage of not amplifying any modes, but at the cost of very weak smoothing. Elman, Ernst and O'Leary [17] proposed using Krylov subspace methods as smoothers. The difficulty here is that different numbers of smoothing steps are necessary at different grid levels, and their optimal determination is challenging.

3.4.2 Coarse Grid Correction

In addition to the finite difference discretization on the mesh

$$\Omega^h := \{x_j = jh : j = 0, \ldots, N+1\}$$

we consider the 1D model problem (15) discretized on a coarser grid

$$\Omega^H := \{x_j = jH : j = 0, \ldots, n+1\}$$

with twice the mesh width $H = 2h$, where $N = 2n+1$. We transfer grid functions $\mathbf{u}^H = [u_1^H, \ldots, u_n^H]$ (we omit the zero boundary values) to the fine grid Ω^h using linear interpolation, which defines the linear mapping

$$I_h^H : \Omega^H \to \Omega^h, \qquad \mathbf{u}^H \mapsto I_h^H \mathbf{u}^H$$

defined by

$$[I_H^h \mathbf{u}^H]_j = \begin{cases} [\mathbf{u}^H]_{j/2} & \text{if } j \text{ is even,} \\ \frac{1}{2}\left([\mathbf{u}^H]_{(j-1)/2} + [\mathbf{u}^H]_{(j+1)/2}\right) & \text{if } j \text{ is odd,} \end{cases} \qquad j = 0,\ldots,N+1, \tag{23}$$

with matrix representation

$$I_H^h = \frac{1}{2}\begin{bmatrix} 1 & & & \\ 2 & & & \\ 1 & 1 & & \\ & 2 & & \\ & 1 & & \\ & & \ddots & 1 \\ & & & 2 \\ & & & 1 \end{bmatrix} \in \mathbb{R}^{N\times n}$$

with respect to the standard unit coordinate bases in $\mathbb{R}^n$ and $\mathbb{R}^N$, respectively.

Following [41], we analyze the mapping properties of the linear interpolation operator I_H^h on the coarse-grid eigenvectors $\{\mathbf{v}_j^H\}_{j=1}^n$ of the discrete 1D Dirichlet-Laplacian , where

$$\mathbf{v}_j^H = [\sin(j\ell\pi H)]_{\ell=1}^n, \qquad j = 1,\ldots,n.$$

Proposition 1. *The coarse-grid eigenvectors are mapped by the interpolation operator I_H^h according to*

$$I_H^h \mathbf{v}_j^H = c_j^2 \mathbf{v}_j^h - s_j^2 \mathbf{v}_{N+1-j}^h, \qquad j = 1,\ldots,n,$$

where we define

$$c_j := \cos\frac{j\pi h}{2}, \quad s_j := \sin\frac{j\pi h}{2}, \qquad j = 1,\ldots,n. \tag{24}$$

In particular, $\mathbf{v}_{n+1}^h$ is not in the range of interpolation.

Proof. For each $j \in \{1,\ldots,n\}$ we distinguish the cases of odd and even index $\ell \in \{1,\ldots,N\}$ corresponding to the two cases in the definition (23). In the first case we obtain using elementary trigonometric identities

$$\begin{aligned} \left[I_H^h \mathbf{v}_j\right]_\ell &= \frac{1}{2}\left([\mathbf{v}_j^H]_{(\ell-1)/2} + [\mathbf{v}_h^H]_{(\ell+1)/2}\right) = \frac{1}{2}\left(\sin\frac{j(\ell-1)\pi H}{2}) + \sin\frac{j(\ell+1)\pi H}{2}\right) \\ &= \frac{1}{2}\Big(\sin(j(\ell-1)\pi h) + \sin(j(\ell+1)\pi h)\Big) = \cos(j\pi h)\sin(j\pi\ell h) \\ &= (c_j^2 - s_j^2)\sin(j\ell\pi h) = c_j^2\sin(j\ell\pi h) - s_j^2\sin((N+1-j)\ell\pi h) \\ &= c_j^2[\mathbf{v}_j^h]_\ell - s_j^2[\mathbf{v}_{N+1-j}^h]_\ell\ . \end{aligned}$$

For even ℓ we obtain

$$\left[I_H^h \mathbf{v}_j\right]_\ell = \left[\mathbf{v}_j^H\right]_{\ell/2} = \sin\frac{j\ell\pi H}{2} = \sin(j\ell\pi h) = (c_j^2 + s_j^2)\sin(j\ell\pi h)$$
$$= c_j^2 \sin(j\ell\pi h) - s_j^2 \sin((N+1-j)\ell\pi h) = c_j^2[\mathbf{v}_j^h]_\ell - s_j^2[\mathbf{v}_{N+1-j}^h]_\ell \,.$$

□

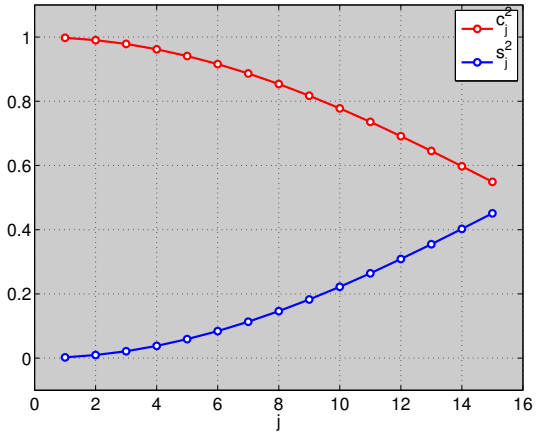

Fig. 13 Coefficients c_j^2 and s_j^2 of the eigenvectors of the discrete 1D Dirichlet-Laplacian under the linear interpolation operator for $N = 31$, i.e., $n = 15$.

The coarse-grid modes $\mathbf{v}_j^H$ are thus mapped to a linear combination of their fine-grid counterparts $\mathbf{v}_j^h$ and a *complementary mode* $\mathbf{v}_{j'}^h$ with index $j' := N+1-j$. Note the relations

$$c_{j'} = s_j \quad s_{j'} = c_j, \qquad j = 1,\ldots,n,$$

between complementary s_j and c_j. Interpolating coarse-grid functions therefore always activates high-frequency modes on the fine grid, with a factor that is less than one but grows with j (cf. Figure 13).

To transfer fine-grid functions to the coarse grid we employ the *full weighting* restriction operator

$$I_h^H : \Omega^h \to \Omega^H, \qquad \mathbf{u}^h \mapsto I_h^H \mathbf{u}^h$$

defined by

$$\left[I_h^H \mathbf{u}^h\right]_j = \frac{1}{4}\Big([\mathbf{u}^h]_{2j-1} + 2[\mathbf{u}^h]_{2j} + [\mathbf{u}^h]_{2j+1}\Big), \qquad j = 1,\ldots,n. \tag{25}$$

The associated matrix representation is given by $I_h^H = \frac{1}{2}[I_H^h]^\top$. The restriction operator is thus seen to be the adjoint of the interpolation operator if one introduces on $\mathbb{R}^n$ and $\mathbb{R}^N$ the Euclidean inner product weighted by the mesh size H and h, respec-

tively. Denoting by $\mathscr{N}(\cdot)$ and $\mathscr{R}(\cdot)$ the null-space and range of a matrix, the basic relation

$$\mathbb{R}^N = \mathscr{R}(I_H^h) \oplus \mathscr{N}([I_H^h]^\top) = \mathscr{R}(I_H^h) \oplus \mathscr{N}(I_h^H) \tag{26}$$

reveals that the range of interpolation and the null-space of the restriction are complementary linear subspaces of $\mathbb{R}^N$, which are also orthogonal with respect to the Euclidean inner product. Since the columns of I_H^h are seen to be linearly independent, the interpolation operator has full rank, which together with (26) implies

$$\dim \mathscr{R}(I_H^h) = n, \qquad \dim \mathscr{N}(I_h^H) = N - n = n + 1.$$

Proposition 2. *The fine-grid eigenvectors are mapped by the restriction operator I_h^H according to*

$$I_h^H \mathbf{v}_j^h = \quad c_j^2 \mathbf{v}_j^H, \qquad j = 1, \ldots, n, \tag{27a}$$

$$I_h^H \mathbf{v}_{N+1-j}^h = -s_j^2 \mathbf{v}_j^H, \qquad j = 1, \ldots, n, \tag{27b}$$

$$I_h^H \mathbf{v}_{n+1}^h = \mathbf{0}. \tag{27c}$$

Proof. By (25) and elementary trigonometric relations we have for $j, \ell \in \{1, \ldots, n\}$

$$\begin{aligned}
\left[I_h^H \mathbf{v}_j^h\right]_\ell &= \frac{1}{4}\left([\mathbf{v}_j^h]_{2\ell-1} + 2[\mathbf{v}_j^h]_{2\ell} + [\mathbf{v}_j^h]_{2\ell+1} \right) \\
&= \frac{1}{4}\left(\sin\left((2\ell-1)j\pi h\right) + 2\sin(2\ell j\pi h) + \sin\left((2\ell+1)j\pi h\right) \right) \\
&= \frac{1}{4}\left(2\sin(2\ell j\pi h) + 2\cos(j\pi h)\sin(2\ell j\pi h) \right) \\
&= \frac{1}{2}\left(1 + \cos(j\pi h) \right) \sin(2\ell j\pi h) \\
&= \cos^2\frac{j\pi h}{2} \sin(\ell j\pi H) = c_j^2 [\mathbf{v}_j^H]_\ell,
\end{aligned}$$

which is (27a). For $j = n+1$ we have $2jh = 1$, implying $\sin(2\ell j\pi h) = 0\ \forall \ell$, which is (27b). To show (27c) note first that

$$[\mathbf{v}_{N+1-j}^h]_\ell = -(-1)^\ell \sin(j\ell\pi h), \qquad j = 1, \ldots, n; \quad \ell = 1, \ldots, N,$$

and therefore

$$\begin{aligned}
\left[I_h^H \mathbf{v}_{N+1-j}^h\right]_\ell &= \frac{1}{4}\left(2\cos(j\pi h)\sin(j\ell\pi H) - (-1)^{2\ell} 2\sin(j\ell\pi H) \right) \\
&= \frac{1}{2}\left(\cos(j\pi h) - 1 \right) \sin(j\ell\pi H) = -\sin^2\frac{j\pi h}{2} \sin(j\ell\pi H) = -s_j^2\, [\mathbf{v}_j^H]_\ell\,.
\end{aligned}$$

□

The coarse-grid correction of an approximation $\mathbf{u}^h$ to the solution of (15) on the fine grid Ω^h is obtained by solving the error equation $A_h\mathbf{e}^h = \mathbf{b} - A_h\mathbf{u}^h = \mathbf{r}^h$ on the coarse grid. To this end, the residual is first restricted to the coarse grid and a coarse-grid representation A_H of the differential operator is used to obtain the approximation $A_H^{-1} I_h^H \mathbf{r}^h$ of the error $A_h^{-1}\mathbf{r}^h$ on Ω^H. The update is then obtained after interpolating this error approximation to Ω^h as

$$\mathbf{u}^h \leftarrow \mathbf{u}^h + I_H^h A_H^{-1} I_h^H (\mathbf{b} - A_h \mathbf{u}^h) \tag{28}$$

with associated error propagation operator

$$C := I - I_H^h A_H^{-1} I_h^H A_h. \tag{29}$$

In view of Propositions 1 and 2 the coarse-grid correction operator C is seen to possess the invariant subspaces

$$\text{span}\{\mathbf{v}_{n+1}^h\} \quad \text{and} \quad \text{span}\{\mathbf{v}_j^h, \mathbf{v}_{j'}^h\}, \quad j' = N+1-j, \qquad j = 1,\ldots,n. \tag{30}$$

Denoting the eigenvalues of the discrete 1D Helmholtz operators on Ω^h and Ω^H by

$$\lambda_j^h = \frac{4}{h^2}\sin^2\frac{j\pi h}{2} - k^2, \qquad j = 1,\ldots,N$$

and

$$\lambda_j^H = \frac{4}{H^2}\sin^2\frac{j\pi H}{2} - k^2, \qquad j = 1,\ldots,n,$$

respectively, the action of the coarse-grid correction operator on these invariant subspaces is given by

$$C\,[\mathbf{v}_j^h\ \mathbf{v}_{j'}^h] = [\mathbf{v}_j^h\ \mathbf{v}_{j'}^h]\,C_j, \qquad j = 1,\ldots,n,$$

where

$$C_j = \begin{bmatrix} 1 & 0 \\ 0 & 1 \end{bmatrix} - \begin{bmatrix} c_j^2 \\ -s_j^2 \end{bmatrix} \frac{1}{\lambda_j^H} \begin{bmatrix} c_j^2 & -s_j^2 \end{bmatrix} \begin{bmatrix} \lambda_j^h & 0 \\ 0 & \lambda_{j'}^h \end{bmatrix} = \begin{bmatrix} 1 - c_j^4 \frac{\lambda_j^h}{\lambda_j^H} & c_j^2 s_j^2 \frac{\lambda_{j'}^h}{\lambda_j^H} \\ c_j^2 s_j^2 \frac{\lambda_j^h}{\lambda_j^H} & 1 - s_j^4 \frac{\lambda_{j'}^h}{\lambda_j^H} \end{bmatrix} \tag{31}$$

in addition to $C\mathbf{v}_{n+1}^h = \mathbf{v}_{n+1}^h$.

For $k = 0$ we observe as in [41]

$$\frac{\lambda_j^h}{\lambda_j^H} = \frac{4s_j^2}{(2s_jc_j)^2} = \frac{1}{c_j^2} \quad \text{as well as} \quad \frac{\lambda_{j'}^h}{\lambda_j^H} = \frac{4c_j^2}{(2s_jc_j)^2} = \frac{1}{s_j^2}, \qquad j = 1,\ldots,n, \tag{32}$$

and therefore

$$C_j = \begin{bmatrix} 1 - c_j^2 & c_j^2 \\ s_j^2 & 1 - s_j^2 \end{bmatrix} = \begin{bmatrix} s_j^2 & c_j^2 \\ s_j^2 & c_j^2 \end{bmatrix}, \qquad j = 1,\ldots,n.$$

A matrix of the form $X = \begin{bmatrix} \xi & \eta \\ \xi & \eta \end{bmatrix}$ has the eigenvalues and spectral norm

$$\Lambda(X) = \{0, \xi + \eta\}, \tag{33a}$$

$$\|X\| = \|XX^\top\|^{1/2} = \sqrt{\xi^2+\eta^2}\left\|\begin{bmatrix} 1 & 1 \\ 1 & 1 \end{bmatrix}\right\|^{1/2} = \sqrt{\xi^2+\eta^2}\cdot\sqrt{2}. \tag{33b}$$

For C_j we thus obtain in the case of the Laplacian

$$\rho(C_j) = s_j^2 + c_j^2 = 1, \quad \|C_j\| = \sqrt{2(s_j^4+c_j^4)}, \qquad j = 1,\ldots,n.$$

From $s_j^2 \in [0, \frac{1}{2}]$ for $j = 1,\ldots,n$ we infer the bound

$$\|C_j\| \le \max_{0\le t\le\frac{1}{2}} \sqrt{2[t^2+(1-t)^2]} = \sqrt{2}, \qquad j = 1,\ldots,n.$$

In the Helmholtz case $k > 0$ the spectral analysis of the coarse grid correction operator C_j becomes more tedious and no simple closed-form expression exists for the spectral radius and norm of the 2×2 blocks C_j. We therefore resort to computation and consider the case of a fine mesh with $N = 31$ interior points. The left of Figure 14 shows a stem plot of the eigenvalues of the 2×2 blocks of C for the Laplacian, which consist of ones and zeros, as C is an orthogonal projection in this case, see (33a). On the right of Figure 14 we see the analogous plot for $k = 6.3\pi$. Note that the unit eigenvalues remain, but that the second eigenvalue of each pair is no longer zero. In particular, mode number 13 is amplified by a factor of nearly -4. This mode is well outside the oscillatory part of the spectrum, so that smoothing cannot be expected to offset such an error amplification. In the example we have shown in

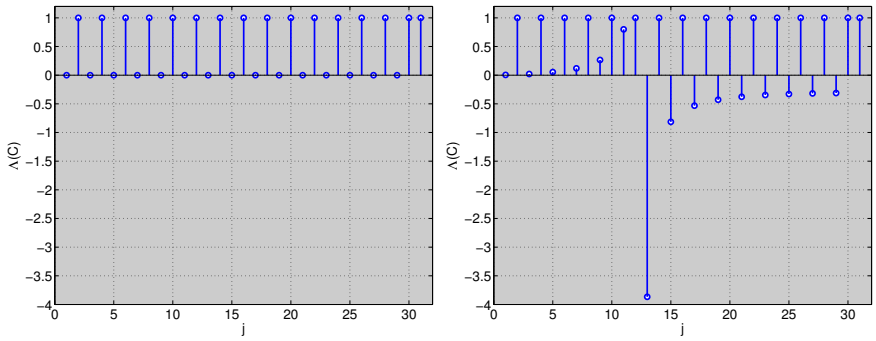

Fig. 14 Eigenvalues of the coarse-grid correction operator with respect to a fine mesh with $h = 1/32$ for $k = 0$ (left) and $k = 6.3\pi$ (right).

Figure 9, we had chosen the parameters precisely such that the corresponding mode

was multiplied by the factor -1, which led to the correct shape of the coarse grid correction, but with the incorrect sign.

A simple device for obtaining a more effective coarse-grid correction for Helmholtz operators results from taking into account the dispersion properties of the discretization scheme. For our uniform centered finite-difference discretization of the 1D Helmholtz operator with constant k

$$\mathscr{L}u \approx \frac{1}{h^2}\left(-u_{j-1}+2u_j-u_{j+1}\right)-k^2u_j,$$

plane-wave solutions $e^{ik^hx_j}$ of the *discrete* homogeneous Helmholtz equation possess a discrete wave number k^h characterized by

$$\frac{k^h}{k}=\frac{1}{kh}\arccos\left(1-\frac{k^2h^2}{2}\right)>1.$$

As a result, the discrete solution exhibits a *phase lead* with respect to the true solution, which grows with h. In the same way, coarse grid approximations in a multigrid hierarchy will be out of phase with fine grid approximations. This suggests 'slowing down' the waves on coarse grids in order that the coarse grid correction again be in phase with the fine grid approximation. For our example, this is achieved by using a modified wave number $\tilde{k}$ in the coarse-grid Helmholtz operator defined by the requirement

$$\tilde{k}^H=k, \quad \text{which is achieved by} \quad \tilde{k}=\sqrt{\frac{2(1-\cos(kh))}{h^2}}.$$

An even better adjustment of the coarse-grid correction results from matching the coarse-grid discrete wave number k^H to the fine-grid discrete wave number k^h by choosing the modified wave number $\tilde{k}$ on the coarse grid to satisfy

$$\tilde{k}^H=k^h \quad \text{which is achieved by} \quad \tilde{k}=k\sqrt{1-k^2h^2/4}. \tag{34}$$

Choosing a modified wave number according to (34) is also equivalent to avoiding a possible 'singularity' in the term λ_j^h/λ_j^H in (31) by forcing the vanishing of λ_j^H as a continuous function of j to occur in the same location as for λ_j^h.

Figure 15 shows the eigenvalues of the coarse-grid correction operator depicted on the right of Figure 14 with the modified wave number (34) used on the coarse grid. The strong amplification of mode number 13 is seen to be much less severe, all non-unit eigenvalues now being less than one in modulus.

Such a dispersion analysis can be carried out for all standard discretization schemes, and it is found that higher order schemes have much lower phase error (cf.,e.g., [3]), making them a favorable choice also from the point of multigrid solvers. In higher dimensions higher order method also possess nearly isotropic dispersion relations, a necessary requirement for (scalar) dispersion correction.

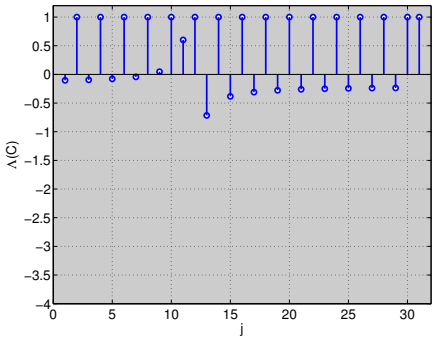

Fig. 15 Eigenvalues of the coarse-grid operator with respect to a fine mesh with $h = 1/32$ for $k = 6.3\pi$ using the modified wave number $\tilde{k}$ given in (34) in the coarse grid Helmholtz operator.

3.4.3 Two-Grid Operator

Two-grid iteration combines one or more smoothing steps with coarse-grid correction. If ν_1 and ν_2 denote the number of *pre-smoothing* and *post-smoothing* steps carried out before and after after coarse-grid correction, the error propagation operator of the resulting *two-grid operator* is obtained as $T = S^{\nu_2} C S^{\nu_1}$. Choosing damped Jacobi iteration with relaxation factor ω as the smoothing operator, the results on the spectral analysis of the damped Jacobi smoother and coarse-grid correction allow us to decompose the analysis of the two-grid operator into the subspaces

$$\operatorname{span}\{\mathbf{v}_1, \mathbf{v}_N\}, \operatorname{span}\{\mathbf{v}_2, \mathbf{v}_{N-1}\}, \ldots, \operatorname{span}\{\mathbf{v}_n, \mathbf{v}_{n+2}\}, \operatorname{span}\{\mathbf{v}_{n+1}\}$$

of n pairs of complementary modes and the remaining 'middle mode' $\mathbf{v}_{n+1}$. The action of T on these one- and two-dimensional subspaces is represented by the block diagonal matrix

$$T = \operatorname{diag}(T_1, \ldots, T_n, T_{n+1})$$

with

$$T_j = \begin{bmatrix} \sigma_j & 0 \\ 0 & \sigma_{j'} \end{bmatrix}^{\nu_2} \begin{bmatrix} 1 - c_j^4 \frac{\lambda_j^h}{\lambda_j^H} & c_j^2 s_j^2 \frac{\lambda_{j'}^h}{\lambda_j^H} \\ c_j^2 s_j^2 \frac{\lambda_j^h}{\lambda_j^H} & 1 - s_j^4 \frac{\lambda_{j'}^h}{\lambda_j^H} \end{bmatrix} \begin{bmatrix} \sigma_j & 0 \\ 0 & \sigma_{j'} \end{bmatrix}^{\nu_1} \qquad j = 1, \ldots, n, \tag{35}$$

and

$$T_{n+1} = (1 - \omega)^{\nu_1 + \nu_2},$$

the latter resulting from $\sigma_{n+1} = 1 - \omega$ (cf. (20)).

We begin again with the case $k = 0$, in which, due to (32), the 2×2 blocks in (35) simplify to (see also [41])

$$T_j = \begin{bmatrix} \sigma_j & 0 \\ 0 & \sigma_{j'} \end{bmatrix}^{\nu_2} \begin{bmatrix} s_j^2 & c_j^2 \\ s_j^2 & c_j^2 \end{bmatrix} \begin{bmatrix} \sigma_j & 0 \\ 0 & \sigma_{j'} \end{bmatrix}^{\nu_1} \quad \text{with} \quad \sigma_j = 1-2\omega s_j^2,\ \sigma_{j'} = 1-2\omega c_j^2.$$

Fixing $\nu_1 = \nu$ and $\nu_2 = 0$ (pre-smoothing only) and $\omega = \omega_0$ (cf. (21)), this becomes

$$T_j = \begin{bmatrix} s_j^2\sigma_j^\nu & c_j^2\sigma_{j'}^\nu \\ s_j^2\sigma_j^\nu & c_j^2\sigma_{j'}^\nu \end{bmatrix}, \quad j = 1,\dots,n, \qquad T_{n+1} = \left(\frac{1}{3}\right)^\nu,$$

where

$$\sigma_j = \frac{1}{3}\left(3-4s_j^2\right), \quad \sigma_{j'} = \frac{1}{3}\left(4s_j^2-1\right), \qquad j = 1,\dots,n.$$

Using (33a) we obtain for the spectral radius

$$\rho(T_j) = s_j^2\sigma_j^\nu + c_j^2\sigma_{j'}^\nu, \quad j = 1,\dots,n, \qquad \rho(T_{n+1}) = 3^{-\nu}.$$

Noting that $c_j^2 = 1-s_j^2$ and $s_j^2 \in [0,\frac{1}{2}]$ for all j, we obtain the upper bound

$$\rho(T_j) \le R_\nu := \max_{0\le t\le\frac{1}{2}} R_\nu(t), \quad R_\nu(t) := t\left(\frac{3-4t}{3}\right)^\nu + (1-t)\left(\frac{4t-1}{3}\right)^\nu$$

for $j = 1,\dots,n$. Since $R_\nu(\frac{1}{2}) = \left(\frac{1}{3}\right)^\nu$ this bound holds also for T_{n+1}. A common upper bound for the spectral norms $\|T_j\|$ is obtained in an analogous way using (33b) as

$$\|T_j\| \le N_\nu := \max_{0\le t\le\frac{1}{2}} N_\nu(t), \quad N_\nu(t) := \sqrt{2\left[t^2\left(\frac{3-4t}{3}\right)^{2\nu} + (1-t)^2\left(\frac{4t-1}{3}\right)^{2\nu}\right]},$$

which holds for all $j = 1\dots,n+1$ due to $N_\nu(\frac{1}{2}) = \left(\frac{1}{3}\right)^\nu$.

$\nu\backslash\rho(T)$	$k=0$	$k=1.3\pi$	$k=4.3\pi$	$k=6.3\pi$
1	0.3333	0.3364	0.4093	0.8857
2	0.1111	0.1170	0.2391	1.8530
3	0.0787	0.0779	0.2623	1.6455
4	0.0617	0.0613	0.2481	1.6349
5	0.0501	0.0493	0.2561	1.5832
10	0.0263	0.0256	0.2668	1.3797

Table 7 Spectral radius of the two-grid operator for the Helmholtz equation with $h = 1/32$ for varying wave number k and (pre-) smoothing step number ν.

Table 7 gives the spectral radius of the two-grid operator for the Helmholtz equation with ν steps of pre-smoothing using damped Jacobi for a range of wave numbers k. We observe that the iteration is divergent for $k = 6.3\pi$, which corresponds to a resolution of roughly 10 points per wavelength. Moreover, while additional

smoothing steps resulted in a faster convergence rate for k close to zero, this is no longer the case for higher wave numbers.

$\nu\backslash\rho(T)$	$k=1.3\pi$	$k=4.3\pi$	$k=6.3\pi$
1	0.3365	0.5050	0.6669
2	0.1173	0.1648	0.1999
3	0.0779	0.1012	0.1542
4	0.0614	0.0568	0.1761
5	0.0493	0.0591	0.2012
10	0.0257	0.0790	0.3916

Table 8 Same as Table 7 using a modified wave number on the coarse grid.

Table (8) gives the spectral radius of the same two-grid operator using the modified wave number according to (34) on the coarse grid. We observe that, even for the unstable damped Jacobi smoother, this results in a convergent two-grid method in this example. A more complete analysis of how far one can get with this approach, and what its limits are, will appear in a forthcoming paper.

3.5 The Shifted Laplacian Preconditioner

An idea proposed in [20], going back to [6], which has received a lot of attention over the last few years, see for example the references in [39], is to precondition the Helmholtz equation (1) using a Helmholtz operator with a rescaled complex wave number,

$$\mathscr{L}_s := -(\Delta + (\alpha + i\beta)k^2), \tag{36}$$

i.e., where damping has been added. The main idea here is that if the imaginary shift β is large enough, standard multigrid methods are known to work again, and, if the shift is not too large and $\alpha \approx 1$, the shifted operator should still be a good preconditioner for the original Helmholtz operator, where $\alpha = 1$ and $\beta = 0$. We show here quantitatively these two contradicting requirements for the one-dimensional case on the unit interval with homogeneous Dirichlet boundary conditions. In that case, both the Helmholtz and the shifted Helmholtz preconditioner can be diagonalized using a Fourier sine series, as we have seen in subsection 3.4, and we obtain for the corresponding symbols (or eigenvalues)

$$\hat{\mathscr{L}} = \frac{2}{h^2}(1-\cos j\pi h) - k^2, \quad \hat{\mathscr{L}_s} = \frac{2}{h^2}(1-\cos j\pi h) - (\alpha+i\beta)k^2, \quad j = 1,\ldots,N.$$

Hence the preconditioned operator $\mathscr{L}_s^{-1}\mathscr{L}$ has the symbol

$$\frac{\hat{\mathscr{L}}}{\hat{\mathscr{L}_s}} = \frac{-2+2\cos j\pi h + h^2k^2}{-2+2\cos j\pi h + h^2k^2(\alpha+i\beta)}.$$

The spectrum of the preconditioned operator therefore lies on a circle in the complex plane, which passes through $(0,0)$, and if $\alpha = 1$, the center is at $(\frac{1}{2},0)$ and the radius equals $\frac{1}{2}$, as one can see using a direct calculation. Examples are shown in Figure 16. Since the circle passes through $(0,0)$ when the numerator of the symbol of the

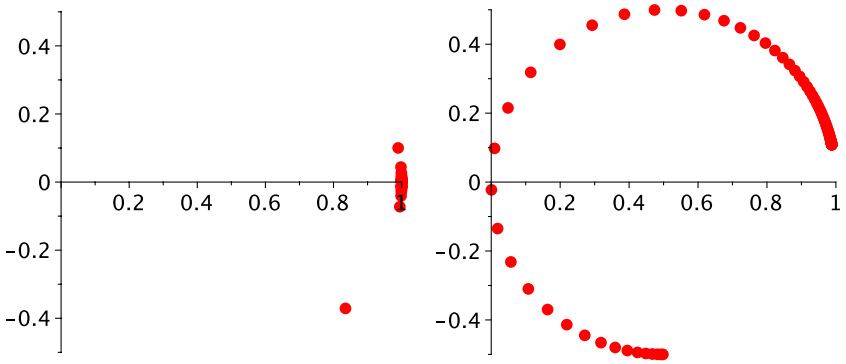

Fig. 16 Spectrum of the Helmholtz operator preconditioned with the shifted Laplacian preconditioner with $\alpha = 0$ and $\beta = 0.01$ on the left, and $\beta = 1$ on the right. The spectrum clustered around the point (1,0) on the left is favorable for a Krylov method, while the spectrum on the right is not, due to the eigenvalues close to zero

preconditioned operator vanishes, i.e.

$$2\cos j\pi h + h^2k^2 = 2, \tag{37}$$

the spectrum of the preconditioned operator is potentially unfavorable for a Krylov method, as one can see in Figure 16 on the right. For $\alpha = 1$ and β small, we have

$$\frac{\hat{\mathscr{L}}}{\hat{\mathscr{L}}_s} = 1 - i\frac{k^2h^2}{-2+2\cos j\pi h + k^2h^2}\beta + O(\beta^2),$$

which shows that the spectrum is clustered on an arc of the circle around $(1,0)$, as illustrated in Figure 16 on the left, provided $\beta \ll \min_{j=1,\ldots,n}|-2+2\cos j\pi h + h^2k^2|$. How small must we therefore choose β ? A direct calculation shows that we must choose $\beta < \frac{1}{k}$ in order to obtain a clustered spectrum about $(1,0)$. We show in Figure 17 an illustration of this fact: from equation (37), we can compute a critical j where the spectrum vanishes,

$$j_c = \frac{1}{\pi h}(\pi - \arccos(-1+\frac{1}{2}k^2h^2)).$$

The spectrum being restricted to integer j, we can plot

$$d := -2 + 2\cos j_c \pi h + k^2 h^2,$$

in order to get an impression of the size of this quantity. We see in Figure 17 that

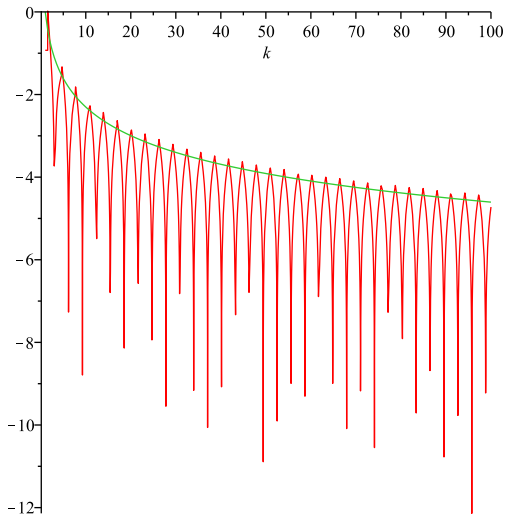

Fig. 17 Illustration of how small β has to be chosen in the shifted Helmholtz preconditioner in order to remain an effective preconditioner for the Helmholtz equation. Note the log scale on the y-axis

the minimum distance d (oscillatory curve in red) behaves like $1/k$ (smooth curve shown in green), and thus β needs to be chosen smaller than $1/k$ for a given problem if one wants to obtain a spectrum of the preconditioned operator close to $(1,0)$.

Now, is it possible to solve the shifted Helmholtz equation effectively with multigrid for this choice of β ? In order to investigate this, we use the two grid analysis from subsection 3.4, now applied to the shifted Laplace problem. We show in Figure 18 the spectral radius of the two grid iteration operator for each frequency pair in (30), for $k = 10, 100, 1000$ using ten points per wavelength, choosing in each case $\beta = 1/k$. This numerical experiment shows clearly that, unfortunately, for the multigrid method to converge when applied to the shifted Laplace operator, β can not be chosen to satisfy $\beta < 1/k$, since already for $\beta = 1/k$ the contraction factor ρ of multigrid grows like $\rho \sim k$ (note the different scaling on the axes in Figure 18) and thus the method is not convergent. One can furthermore show that β must be a constant, independent of k, in order to obtain a contraction factor $\rho < 1$ and a convergent multigrid algorithm. Hence the shifted Laplacian preconditioner might not be an effective choice to solve large scale Helmholtz problems, in particular when the wave number k becomes large.

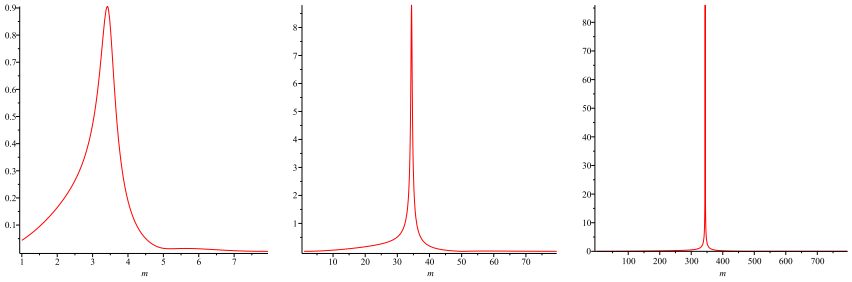

Fig. 18 Spectral radius of the two grid iteration operator for all frequency pairs. On the left for $k = 10$, in the middle for $k = 100$ and on the right for $k = 1000$, with the shift $\beta = 1/k$ in order to guarantee a spectrum away from $(0,0)$ of the Helmholtz operator preconditioned by the shifted Laplace preconditioner

3.6 Wave-Ray Multigrid

In [9] Brandt and Livshits proposed a variant of multigrid especially tailored to the Helmholtz equation by exploiting the structure of the error components which standard multigrid methods fail to eliminate. These are the so-called *characteristic components*, which are discrete representations of functions of the form

$$u(x,y) = v(x,y)e^{ik_1x+ik_2y}, \qquad k_1^2 + k_2^2 = k^2. \tag{38}$$

Such factorizations are common in geometrical optics (see, e.g. [47, 49]), and from there the terminology *ray function* for the amplitude term $v(x,y)$ and *phase* for the exponent $k_1x + k_2y$ is adopted. Characteristic components of the error are nearly invisible to standard smoothing techniques since they have very small residuals on grids which resolve these oscillations. On coarser grids they are contaminated by phase errors and ultimately by approximation errors.

The ray functions, however, are smooth, and satisfy a convection-diffusion-type PDE, called the *ray equation*, which is obtained by inserting (38) into the Helmholtz equation. In their *wave-ray multigrid method*, Brandt and Livshits add so-called *ray cycles* to the standard multigrid scheme, in which the ray functions of principal components are approximated by performing smoothing with respect to the ray equation on auxiliary grids which they call *ray grids*.

We describe the basic idea for the simple 1D model problem (15) with constant wave number k as first described in Livshits' Ph.D. thesis [52]. Multidimensional generalizations such as described in [9] introduce a considerable number of technical and algorithmic complications. In 1D principal error components have the form

$$v(x) = a(x)e^{ikx} + b(x)e^{-ikx},$$

which, when inserted into the homogeneous Helmholtz equation, yields the equation

$$\left(a''(x) + 2ika'(x)\right)e^{ikx} + \left(b''(x) - 2ikb'(x)\right)e^{-ikx} = 0$$

which we separate into

$$L_+ a = a'' + 2ika' = 0, \qquad L_- b = b'' - 2ikb' = 0.$$

The wave-ray method employs a standard multigrid scheme, say, a V-cycle, to first eliminate the non-characteristic components from the error $\mathbf{e}^h$, such that the associated residual $\mathbf{r}^h = A^h \mathbf{e}^h$ is approximately of the form

$$\mathbf{r}_j^h = (r_a^h)_j e^{ikx_j} + (r_b^h)_j e^{-ikx_j},$$

with smooth ray grid functions r_a^h and r_b^h. By a process called *separation* the two components of the residual are first isolated, resulting in the right hand sides of the two ray equations

$$L_+^h a^h = f_+^h, \quad L_-^h b^h = f_b^h,$$

which are each solved on separate grids and then used to construct a correction of the current approximation.

Details of the separation technique, the treatment of multidirectional rays necessary for higher space dimensions, suitable cycling schedules as well as the incorporation of radiation boundary conditions can be found in [52, 9].

4 Conclusions

Solving the indefinite Helmholtz equation by iterative methods is a difficult task. In all classical methods, the special oscillatory and non-local structure of the associated Green's function leads to severe convergence problems. Specialized methods exist for all well known classes of iterative methods, like preconditioned Krylov methods by incomplete factorizations, domain decomposition and multigrid, but they need additional components tailored for the indefinite Helmholtz problem, which can become very sophisticated and difficult to implement, especially if one wants to achieve a performance independent of the wave number k.

Acknowledgements The authors would like to acknowledge the support of the Swiss National Science Foundation Grant number 200020-121828.

References

1. Y. Achdou and F. Nataf. Dimension-wise iterated frequency filtering decomposition. *Num. Lin. Alg. and Appl.*, 41(5):1643–1681, 2003.
2. Y. Achdou and F. Nataf. Low frequency tangential filtering decomposition. *Num. Lin. Alg. and Appl.*, 14:129–147, 2007.
3. Mark Ainsworth. Discrete dispersion relation for *hp*-version finite element approximation at high wave number. *SIAM J. Numer. Anal.*, 42(2):553–575, 2004.

4. S. McCormick B. Lee, T. Manteuffel and J. Ruge. First-order system least squares (FOSLS) for the Helmholtz equation. *SIAM J. Sci. Comp.*, 21:1927–1949, 2000.
5. N.S. Bakhvalov. Convergence of one relaxation method under natural constraints on the elliptic operator. *Zh. Vychisl. Mat. Mat. Fiz.*, 6:861–883, 1966.
6. A. Bayliss, C.I. Goldstein, and E. Turkel. An iterative method for the Helmholtz equation. *J. Comput. Phys.*, 49:443–457, 1983.
7. T. Betcke, S.N., Chandler-Wilde, I.G. Graham, S. Langdon, and M. Lindner. Condition number estimates for combined potential operators in acoustics and their boundary element discretisation. *Numerical Methods for PDEs*, 27(1):31–69, 2010.
8. A. Brandt and S. Ta'asan. Multigrid methods for nearly singular and slightly indefinite problems. In *Multigrid Methods II*, pages 99–121. Springer, 1986.
9. Achi Brandt and Irene Livshits. Wave-ray multigrid method for standing wave equations. *Electron. Trans. Numer. Anal.*, 6:162–181, 1997.
10. William L. Briggs and Van Emden Henson ans Steve F. McCormick. *A Multigrid Tutorial*. SIAM, 2000.
11. B. Buzbee, F. W. Dorr, J. A. George, and G. Golub. The direct solution of the discrete Poisson equation on irregular regions. *SIAM J. Numer. Anal.*, 8:722–736, 1974.
12. A. Buzdin. Tangential decomposition. *Computing*, 61:257–276, 1998.
13. D. Colton and R. Kress. *Integral Equation Methods in Scattering Theory*. Wiley, New York, 1983.
14. L. Debreu and E. Blayo. On the Schwarz alternating method for ocean models on parallel computers. *J. Computational Physics*, 141:93–111, 1998.
15. B. Després. *Méthodes de décomposition de demains pour les problèms de propagation d'ondes en régime harmonique*. PhD thesis, Université Paris IX Dauphine, 1991.
16. Boris Diskin, 2001. Personal Communication.
17. Howard C. Elman, Oliver G. Ernst, and Dianne P. O'Leary. A multigrid method enhanced by Krylov subspace iteration for discrete Helmholtz equations. *SIAM J. Sci. Comp.*, 23:1290–1314, 2001.
18. B. Engquist and Lexing Ying. Sweeping preconditioner for the Helmholtz equation: Hierarchical matrix representation. *Preprint*, 2010.
19. B. Engquist and Lexing Ying. Sweeping preconditioner for the Helmholtz equation: Moving perfectly matched layers. *Preprint*, 2010.
20. Y.A. Erlangga, C. Vuik, and C.W. Oosterlee. On a class of preconditioners for solving the Helmholtz equation. *Applied Numerical Mathematics*, 50:409–425, 2004.
21. Oliver G. Ernst. *Fast Numerical Solution of Exterior Helmholtz Problems with Radiation Boundary Condition by Imbedding*. PhD thesis, Stanford University, 1994.
22. Oliver G. Ernst. A finite element capacitance matrix method for exterior Helmholtz problems. *Numer. Math.*, 75:175–204, 1996.
23. Oliver G. Ernst. Residual-minimizing Krylov subspace methods for stabilized discretizations of convection-diffusion equations. *SIAM J. Matrix Anal. Appl.*, 22(4):1079–1101, 2000.
24. C. Farhat, P. Avery, R. Tezaur, and J. Li. FETI-DPH: a dual-primal domain decomposition method for accoustic scattering. *Journal of Computational Acoustics*, 13:499–524, 2005.
25. Charbel Farhat, Philip Avery, Radek Tesaur, and Jing Li. FETI-DPH: a dual-primal domain decomposition method for acoustic scattering. *Journal of Computational Acoustics*, 13(3):499–524, 2005.
26. Charbel Farhat, Antonini Macedo, and Radek Tezaur. FETI-H: a scalable domain decomposition method for high frequency exterior Helmholtz problem. In Choi-Hong Lai, Petter Bjørstad, Mark Cross, and Olof Widlund, editors, *Eleventh International Conference on Domain Decomposition Method*, pages 231–241. DDM.ORG, 1999.
27. Charbel Farhat and Francois-Xavier Roux. A method of Finite Element Tearing and Interconnecting and its parallel solution algorithm. *Int. J. Numer. Meth. Engrg.*, 32:1205–1227, 1991.
28. R.P. Federenko. A relaxation method for solving elliptic difference equations. *USSR Comput. Math. and Math. Phys.*, 1(5):1092–1096, 1961.

29. M. J. Gander and F. Nataf. AILU: A preconditioner based on the analytic factorization of the elliptic operator. *Num. Lin. Alg. and Appl.*, 7(7-8):543–567, 2000.
30. Martin J. Gander. Optimized Schwarz methods. *SIAM J. Numer. Anal.*, 44(2):699–731, 2006.
31. Martin J. Gander. Schwarz methods over the course of time. *Electronic Transactions on Numerical Analysis (ETNA)*, 31:228–255, 2008.
32. Martin J. Gander, Laurence Halpern, and Frédéric Magoulès. An optimized Schwarz method with two-sided robin transmission conditions for the Helmholtz equation. *Int. J. for Num. Meth. in Fluids*, 55(2):163–175, 2007.
33. Martin J. Gander, Laurence Halpern, and Frédéric Nataf. Optimized Schwarz methods. In Tony Chan, Takashi Kako, Hideo Kawarada, and Olivier Pironneau, editors, *Twelfth International Conference on Domain Decomposition Methods, Chiba, Japan*, pages 15–28, Bergen, 2001. Domain Decomposition Press.
34. Martin J. Gander, Frédéric Magoulès, and Frédéric Nataf. Optimized Schwarz methods without overlap for the Helmholtz equation. *SIAM J. Sci. Comput.*, 24(1):38–60, 2002.
35. Martin J. Gander, Veronique Martin, and Jean-Paul Chehab. GMRES convergence analysis for diffusion, convection diffusion and Helmholtz problems. *In preparation*, 2011.
36. Martin J. Gander and Frédéric Nataf. An incomplete LU preconditioner for problems in acoustics. *Journal of Computational Acoustics*, 13(3):1–22, 2005.
37. Martin J. Gander and Gerhard Wanner. From Euler, Ritz and Galerkin to modern computing. *Submitted*, 2010.
38. Martin J. Gander and Hui Zhang. Domain decomposition methods for Helmholtz problems: a systematic numerical comparison. *in preparation*, 2011.
39. M.B. Van Gijzen, Y.A. Erlangga, and C. Vuik. Spectral analysis of the discrete Helmholtz operator preconditioned with a shifted Laplacian. *SIAM J. Sci. Comput.*, 29(5):1942–1958, 2007.
40. E. Giladi and J. B. Keller. Iterative solution of elliptic problems by approximate factorization. *Journal of Computational and Applied Mathematics*, 85:287–313, 1997.
41. Wolfgang Hackbusch. *Multi-Grid Methods and Applications*. Springer-Verlag, 1985.
42. Thomas Hagstrom, R. P. Tewarson, and Aron Jazcilevich. Numerical experiments on a domain decomposition algorithm for nonlinear elliptic boundary value problems. *Appl. Math. Lett.*, 1(3), 1988.
43. E. Heikkola, J. Toivanen, and T. Rossi. A parallel fictitious domain method for the three-dimensional Helmholtz equation. *SIAM J. Sci. Comput*, 24(5):1567–1588, 2003.
44. Morton A. Hyman. Non-iterative numerical solution of boundary-value problems. *Appl. Sci. Res. Sec. B2*, 2:325–351, 1952.
45. Frank Ihlenburg and Ivo Babuška. Finite element solution to the Helmholtz equation with high wave number. Part I: The *h*-version of the FEM. *Computer Methods in Applied Mechanics and Engineering*, 39:9–37, 1995.
46. Frank Ihlenburg and Ivo Babuška. Finite element solution to the Helmholtz equation with high wave number. Part II: The *h*-*p* version of the FEM. *SIAM Journal on Numerical Analysis*, 34:315–358, 1997.
47. Joseph B. Keller. Rays, waves and asymptotics. *Bull. Amer. Math. Soc.*, 84(5):727–750, 1978.
48. Lance M. Leslie and Bryant J. McAveney. Comparative test of direct and iterative methods for solving Helmholtz-type equations. *Mon. Wea. Rev.*, 101:235–239, 1973.
49. Robert M. Lewis. Asymptotic theory of wave-propagation. *Archive for Rational Mechanics and Analysis*, 20(3):191–250, 1965.
50. Jörg Liesen and Zdenek Strakoš. GMRES convergence analysis for a convection-diffusion model problem. *SIAM J. Sci. Comput*, 26(6):1989–2009, 2005.
51. Pierre-Louis Lions. On the Schwarz alternating method. III: a variant for nonoverlapping subdomains. In Tony F. Chan, Roland Glowinski, Jacques Périaux, and Olof Widlund, editors, *Third International Symposium on Domain Decomposition Methods for Partial Differential Equations , held in Houston, Texas, March 20-22, 1989*, Philadelphia, PA, 1990. SIAM.
52. Irene Livshits. *Multigrid Solvers for Wave Equations*. PhD thesis, Bar-Ilan University, Ramat-Gan, Israel, 1996.

53. F. Nataf. Résolution de l'équation de convection-diffusion stationaire par une factorisation parabolique. *C. R. Acad. Sci.*, I 310(13):869–872, 1990.
54. Q. Niu, L. Grigori, P. Kumar, and F. Nataf. Modified tangential frequency filtering decomposition and its Fourier analysis. *Numerische Mathematik*, 116(1), 2010.
55. W. Proskurowski and O. B. Widlund. On the numerical solution of Helmholtz's equation by the capacitance matrix method. *Math. Comp.*, 30:433–468, 1976.
56. Thomas E. Rosmond and Frank D. Faulkner. Direct solution of elliptic equations by block cyclic reduction and factorization. *Mon. Wea. Rev.*, 104:641–649, 1976.
57. Y. Saad. *Iterative Methods for Sparse Linear Systems*. PWS Publishing Company, 1996.
58. V. Saul'ev. On solution of some boundary value problems on high performance computers by fictitious domain method. *Siberian Math. J.*, 4:912–925, 1963 (in Russian).
59. H. A. Schwarz. Über einen Grenzübergang durch alternierendes Verfahren. *Vierteljahrsschrift der Naturforschenden Gesellschaft in Zürich*, 15:272–286, May 1870.
60. Richard Vynne Southwell. *Relaxation Methods in Theoretical Physics*. Oxford University Press, 1946.
61. Eduart Stiefel. Über einige Methoden der Relaxationsrechnung. *Z. Angew. Math. Phys.*, 3:1–33, 1952.
62. C. Wagner. Tangential frequency filtering decompositions for symmetric matrices. *Numer. Math.*, 78(1):119–142, 1997.
63. C. Wagner. Tangential frequency filtering decompositions for unsymmetric matrices. *Numer. Math.*, 78(1):143–163, 1997.
64. G. Wittum. An ILU-based smoothing correction scheme. In *Parallel algorithms for partial differential equations*, volume 31, pages 228–240. Notes Numer. Fluid Mech., 1991. 6th GAMM-Semin., Kiel/Ger.
65. G. Wittum. *Filternde Zerlegungen. Schnelle Löser für grosse Gleichungssysteme*. Teubner Skripten zur Numerik, Stuttgart, 1992.
66. E. Zauderer. *Partial Differential Equations of Applied Mathematics*. John Wiley & Sons, second edition, 1989.